

Flavor changing Z-decays from scalar interactions at a Giga-Z Linear Collider

David Atwood*

Department of Physics and Astronomy, Iowa State University, Ames, IA 50011, USA

Shaouly Bar-Shalom†

Theoretical Physics Group, Rafael, Haifa 31021, Israel

Gad Eilam‡

Physics Department, Technion-Institute of Technology, Haifa 32000, Israel

Amarjit Soni§

Theory Group, Brookhaven National Laboratory, Upton, NY 11973, USA

(Dated: October 26, 2018)

The flavor changing decay $Z \rightarrow d_I \bar{d}_J$ is investigated with special emphasis on the $b\bar{s}$ final state. Various models for flavor violation are considered: two Higgs doublet models (2HDM's), supersymmetry (SUSY) with flavor violation in the up and down-type squark mass matrices and SUSY with flavor violation mediated by R -parity-violating interaction. We find that, within the SUSY scenarios for flavor violation, the branching ratio for the decay $Z \rightarrow b\bar{s}$ can reach 10^{-6} for large $\tan\beta$ values, while the typical size for this branching ratio in the 2HDM's considered is about two orders of magnitudes smaller at best. Thus, flavor changing SUSY signatures in radiative Z decays such as $Z \rightarrow b\bar{s}$ may be accessible to future “Z factories” such as a Giga-Z version of the TESLA design.

PACS numbers: 13.38.-b, 12.60.-i, 14.70.-e, 12.60.Jv

I. INTRODUCTION

Rare processes involving various particles have always been a gold mine for extracting interesting physics [1, 2]. For example, the smallness of Flavor Changing Neutral Currents (FCNC) in the K system prompted the introduction of the GIM mechanism and subsequently to the prediction $m_c \approx 1.5$ GeV and the discovery of J/Ψ and D 's. $B\bar{B}$ mixing was a precursor to a heavy top quark, as confirmed by experiment. FCNC rare top decays, for which there are only weak upper bounds, will hopefully be discovered in future experiments, thus serving as direct indications for deviations from the Standard Model (SM), since the latter leads to branching ratios which are smaller than 10^{-10} .

The situation in rare Z decays, which is the subject of this paper, bears some similarities to rare t decays. In both cases the SM results from the loop induced FCNC decays are very small, beyond reach, at least for t , in the foreseeable future. Therefore, any significant detection of a rare decay at the level higher than 10^{-10} or 10^{-8} for t or Z , respectively, would serve as an indisputable proof for physics beyond the SM. If new physics is “around the corner”, *i.e.* at ≈ 1 TeV, the Z boson and the top being so close to that scale, are expected to be

the particles most affected by new physics.

In this paper we study the rare decays $Z \rightarrow d_I \bar{d}_J$, where I, J indicate the generation index of a charge $-1/3$ quark, in various models. In the SM it was found that [3] $\text{Br}(Z \rightarrow b\bar{s} + \bar{b}s) \sim 10^{-8}$; we do not repeat the SM calculation here. Three of the models we discuss, have already been considered in connection with $Z \rightarrow b\bar{s}$, namely the 2 Higgs Doublets Model type II (2HDMII) [4], Supersymmetry (SUSY) [5] and SUSY with R-Parity Violation (RPV) [6]. Therefore we comment, wherever it is relevant in the coming sections, about differences and similarities with previous works. Note that in addition one can find in the literature discussion of FCNC hadronic Z decays, in models not covered by us in the present article [7].

Experimentally, the attention devoted to FCNC in Z decays at LEP and SLD has been close to nil. The best upper limit is [8]

$$\sum_{q=d,s} \text{Br}(Z \rightarrow b\bar{q}) \leq 1.8 \times 10^{-3} \text{ at } 90\% \text{ CL} . \quad (1)$$

This preliminary result is based on about 3.5×10^6 hadronic decays, and we used [9] $\text{Br}(Z \rightarrow \text{hadrons}) = 0.7$. We urge our experimental colleagues to sift through their LEP data to improve the current, rather loose, limit.

In the future, there will be at least two venues in which Z bosons will be produced in much larger quantities than their number in LEP. In a high luminosity LHC with an integrated luminosity of 100 fb^{-1} , one expects 5.5×10^9 Z bosons to be produced [10]. A cleaner environment for the processes at hand, will be provided by a future

*Electronic address: atwood@iastate.edu

†Electronic address: shaouly@physics.technion.ac.il

‡Electronic address: eilam@physics.technion.ac.il

§Electronic address: soni@bnl.gov

e^+e^- linear collider. In particular, there is a viable possibility to lower the TESLA center of mass energy down to $\sqrt{s} = m_Z$, the so called ‘‘Giga-Z’’ option. With integrated luminosity of 30 fb^{-1} , it is possible to produce more than 10^9 Z bosons [11], about 2 orders of magnitudes larger than in LEP. To grasp the improvement in going from LEP to Giga-Z option of TESLA, we note that while the sensitivity of LEP to $Z \rightarrow \tau\mu$ was $\approx 10^{-5}$ [9], it is expected to be $\approx 10^{-8}$ in Giga-Z TESLA [11].

Beyond LHC and the e^+e^- linear collider, there is also considerable interest in the community for a high energy muon collider [12]. If this ever becomes a reality, it would also afford another very good opportunity for studying rare flavor changing decays and interactions [13].

The paper is organized as follows: In Section 2 we present a generic calculation of the $Zd_I\bar{d}_J$ vertex at the one loop level. This result will assist us to evaluate the branching ratio for the FCNC Z decays in any particular model. In Section 3, the results of two variants of the Two Higgs Doublets Model (2HDM), namely the so called type II 2HDM (2HDMII) and the Top-Higgs Two Doublets Model (T2HDM), will be reported. In 2HDMII, T2HDM we get the disappointing results $\text{Br}(Z \rightarrow b\bar{s} + \bar{b}s) \sim 10^{-10}$, 10^{-8} , respectively. We then move on to Section 4, where our results in Supersymmetry (SUSY) with squark mixing, are displayed. Again, two options are presented, the first one with $\tilde{b}-\tilde{s}$ mixing and the second one with $\tilde{t}-\tilde{c}$ mixing. In the first case the branching ratio can reach a respectable $\text{Br}(Z \rightarrow b\bar{s} + \bar{b}s) \sim 10^{-6}$ while the second case yields a branching ratio of $\mathcal{O}(10^{-8})$. In Section 5 we turn to SUSY with R-parity violation (RPV), where the effects of λ' trilinear coupling terms in the RPV superpotential and of b terms (b is the coefficient of the soft breaking RPV bilinear term), are considered. Two categories of RPV are considered: Those which lead to a branching ratio $\propto \lambda' \times \lambda'$ and those with a branching ratio $\propto b\lambda'$. For the first category we get typically branching ratios at the level of 10^{-10} , while for the second type of RPV, we find an encouraging possibility of $\text{Br}(Z \rightarrow b\bar{s} + \bar{b}s) \sim 10^{-6}$. Finally, in Section 6 we summarize our results.

II. GENERIC SCALAR CALCULATION

In this section we outline the generic framework for calculating the radiative one-loop flavor changing interaction vertex $Vd_I\bar{d}_J$ with $I \neq J$ and $V = Z$ or γ . We define the one-loop amplitude for $V \rightarrow d_I\bar{d}_J$ in terms of form factors which are calculated for the complete set of one-loop diagrams that can potentially contribute to $V \rightarrow d_I\bar{d}_J$ in the presence of flavor violating interactions between neutral scalars and fermions as well as non-diagonal vertices of charged scalars with fermions of different generations.

The diagrams that modify (at one loop) the $Vd_I\bar{d}_J$ coupling due to charged or neutral scalar exchanges are depicted in Fig. 1.

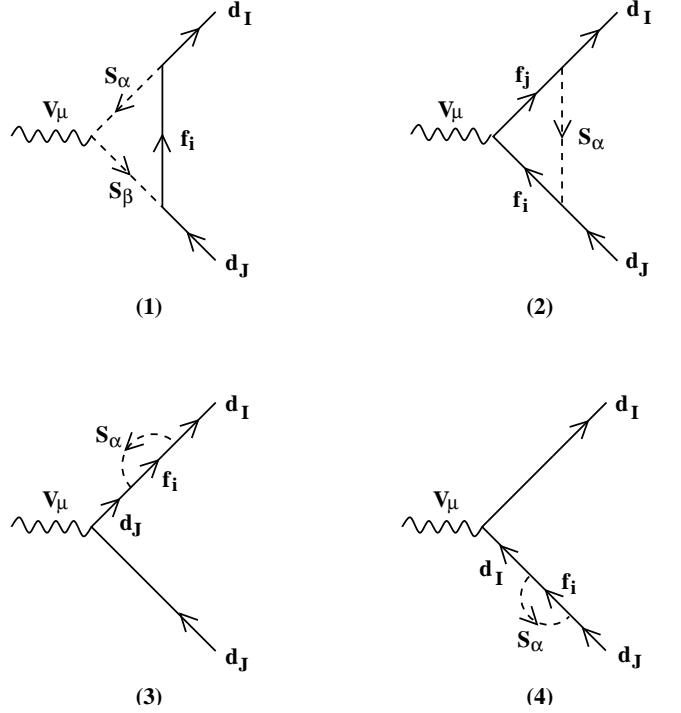


FIG. 1: One-loop diagrams that contribute to the flavor changing transition $V \rightarrow d_I\bar{d}_J$, due to scalar-fermion exchanges.

In what follows, we will denote the internal scalars (S) in the loops by Greek letters and fermions (f) will be given Latin indices i, j .

From Fig. 1 it is evident that we have only three types of interaction vertices to consider. These are defined as follows:

1. $V_\mu - f_i - \bar{f}_j$ interaction

$$i\gamma_\mu \left(a_{L(Vf)}^{ij} L + a_{R(Vf)}^{ij} R \right) \quad (2)$$

where $L(R) = (1-(+)\gamma_5)/2$. For the case of the SM couplings of a vector boson V to a pair of fermions, i.e., $f = u$ (up-quark) or $f = d$ (down-quark), there are only diagonal Vff couplings. In this case we have:

$$a_{L,R(Vf)}^{ij} (i = j) \equiv a_{L,R(Vf)} . \quad (3)$$

where

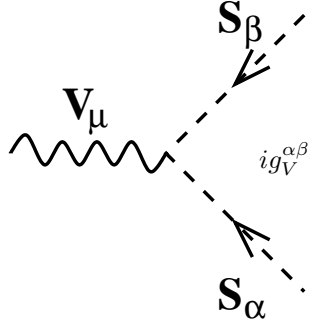
$$a_{L,R(Zf)} = -g_Z \left(T_{L,R}^{3(f)} - s_W^2 Q_f \right) , \quad (4)$$

$$a_{L(\gamma f)} = a_{R(\gamma f)} = -g_\gamma Q_f , \quad (5)$$

with $T_L^{3(u)} = 1/2$ and $T_L^{3(d)} = -1/2$ for an up and down-quark, respectively, and $T_R^{3(f)} = 0$. Also, Q_f is the charge of f and

$$g_Z = \frac{e}{s_W c_W} , \quad g_\gamma = e . \quad (6)$$

2. $V_\mu - S_\alpha - S_\beta$ interaction

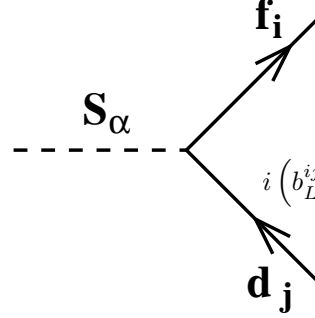


$$i g_V^{\alpha\beta} (p_\alpha - p_\beta)_\mu \quad (7)$$

where S_α and S_β are charged or neutral spin 0 par-

ticles with incoming 4-momenta p_α and p_β , respectively.

3. $S_\alpha - \bar{f}_i - d_j$ interaction



$$i \left(b_{L(\alpha)}^{ij} L + b_{R(\alpha)}^{ij} R \right) \quad (8)$$

where d is a down-quark.

The one-loop amplitudes \mathcal{M}_k ($k = 1, 2, 3, 4$ corresponding to diagrams 1, 2, 3, 4 in Fig. 1, respectively), for the decay $V \rightarrow d_I \bar{d}_J$ can be parametrized generically as follows:

$$\mathcal{M}_k^{IJ} \equiv \frac{i}{16\pi^2} \epsilon_\mu^V(q) \bar{u}_{d_I}(p_I) \left\{ \gamma^\mu \left(A_{L,k}^{IJ} L + A_{R,k}^{IJ} R \right) + \left(B_{L,k}^{IJ} L + B_{R,k}^{IJ} R \right) p_I^\mu \right\} v_{\bar{d}_J}(p_J) , \quad (9)$$

where $\epsilon^V(q)$ is the polarization vector of V , q is its 4-momenta and \bar{u}_{d_I} ($v_{\bar{d}_J}$) is the Dirac spinor of the outgoing d_I with 4-momenta p_I (\bar{d}_J with 4-momenta p_J) such that $q = p_I + p_J$. Also, $A_{L,k}^{IJ}$, $A_{R,k}^{IJ}$, $B_{L,k}^{IJ}$, $B_{R,k}^{IJ}$ are momentum dependent form factors.

Using the Feynman rules in (2), (7) and (8), these form factors can be readily calculated for each diagram. Neglecting terms of $\mathcal{O}(m_b/\sqrt{q^2})$ we get:

$$A_{L,1}^{IJ} = -2 \sum_{\alpha,\beta,i} g_V^{\alpha\beta} b_{L(\alpha)}^{iI} b_{L(\beta)}^{iJ} C_{24}^1 , \quad (10)$$

$$B_{L,1}^{IJ} = 2 \sum_{\alpha,\beta,i} \hat{P}_i m_{f_i} g_V^{\alpha\beta} b_{R(\alpha)}^{iI} b_{L(\beta)}^{iJ} (C_0^1 + C_{11}^1) , \quad (11)$$

$$A_{L,2}^{IJ} = -2 \sum_{\alpha,i,j} b_{L(\alpha)}^{iI} b_{L(\alpha)}^{jJ} \left\{ a_{R(Vf)}^{ij} [p_I \cdot p_J (C_{23}^2 - C_{22}^2) - C_{24}^2] + \hat{P}_i \hat{P}_j m_{f_i} m_{f_j} a_{L(Vf)}^{ij} C_0^2 \right\} , \quad (12)$$

$$B_{L,2}^{IJ} = -2 \sum_{\alpha,i,j} b_{R(\alpha)}^{iI} b_{L(\alpha)}^{jJ} \left\{ \hat{P}_i m_{f_i} a_{L(Vf)}^{ij} (C_{11}^2 - C_{12}^2) + \hat{P}_j m_{f_j} a_{R(Vf)}^{ij} C_{12}^2 \right\} , \quad (13)$$

where $\hat{P}_i = -1$ if the internal fermion in the loop is a charged conjugate state (f_i^c) or else $\hat{P}_i = 1$.

Combining the contribution of the two self energy diagrams, i.e., $\mathcal{M}_3 + \mathcal{M}_4 \equiv \mathcal{M}_{34}$, and similarly for the form factors, e.g., $A_{L,3}^{IJ} + A_{L,4}^{IJ} \equiv A_{L,34}^{IJ}$ etc., we have:

$$A_{L,34}^{IJ} = a_{L(Vd)} \sum_{\alpha,i} b_{L(\alpha)}^{iI} b_{L(\alpha)}^{iJ} B_1^3, \quad (14)$$

$$B_{L,34}^{IJ} = 0. \quad (15)$$

The right-handed form factors, $A_{R,k}^{IJ}$ and $B_{R,k}^{IJ}$, are obtained from the corresponding left handed ones, $A_{L,k}^{IJ}$ and $B_{L,k}^{IJ}$ respectively, by interchanging $L \rightarrow R$ and $R \rightarrow L$ in all the couplings which appear in (10)-(15).

The three-point one-loop form factors C_x^k with $x \in 0, 11, 12, 21, 22, 23, 24$, and two-point form factors B_x^k with $x \in 0, 1$, correspond to the loop integrals of dia-

grams $k = 1 - 4$ and are given by:

$$C_x^1 = C_x \left(m_{f_i}^2, m_{S_\alpha}^2, m_{S_\beta}^2, m_{d_I}^2, q^2, m_{d_J}^2 \right), \quad (16)$$

$$C_x^2 = C_x \left(m_{S_\alpha}^2, m_{f_i}^2, m_{f_j}^2, m_{d_J}^2, q^2, m_{d_I}^2 \right), \quad (17)$$

$$B_x^3 = B_x \left(m_{f_i}^2, m_{S_\alpha}^2, m_{d_I}^2 \right), \quad (18)$$

where $B_x(m_1^2, m_2^2, p^2)$ and $C_x(m_1^2, m_2^2, m_3^2, p_1^2, p_2^2, p_3^2)$ are defined in the appendix.

In terms of the above form factors, the partial width for the decay $Z \rightarrow d_I \bar{d}_J$ is:

$$\Gamma(Z \rightarrow d_I \bar{d}_J) = \frac{N_C}{3} \left(\frac{1}{16\pi^2} \right)^2 \frac{M_Z}{16\pi} \times \left[2 \left(|A_L^T|^2 + |A_R^T|^2 \right) + \frac{M_Z^2}{4} \left(|B_L^T|^2 + |B_R^T|^2 \right) \right], \quad (19)$$

where $N_C = 3$ is the color factor and

$$A_P^T \equiv A_{P,1}^{IJ} + A_{P,2}^{IJ} + A_{P,34}^{IJ}, \quad (20)$$

$$B_P^T \equiv B_{P,1}^{IJ} + B_{P,2}^{IJ} + B_{P,34}^{IJ}, \quad (21)$$

for $P = L$ and R .

III. TWO HIGGS DOUBLETS MODELS

In a 2HDM with flavor diagonal couplings of the neutral Higgs to down-quarks, the flavor changing decay $Z \rightarrow d_I \bar{d}_J$ proceeds through the one-loop diagrams in Fig. 1.

The interaction vertices required for the calculation of the form factors defined in (9) in such models are:

$$\begin{aligned} V_\mu f_i \bar{f}_j &\rightarrow Z_\mu u_i \bar{u}_j, \\ V_\mu S_\alpha S_\beta &\rightarrow Z_\mu H^+ H^-, \\ S_\alpha \bar{f}_i d_j &\rightarrow H^+ \bar{u}_i d_j, \end{aligned} \quad (22)$$

where the $Z_\mu u_i \bar{u}_j$ coupling is the SM one as given in (3)-(6), $S_1 = H^+$ is the only charged Higgs present in this type of models and $f_i = u_i$, $i = 1, 2, 3$ for the three up-type quarks $u_1 = u$, $u_2 = c$, $u_3 = t$.

The $Z_\mu H^+ H^-$ coupling is obtained from the scalar kinetic term $(D^\mu \Phi_i)^\dagger (D_\mu \Phi_i)$, where $\Phi_{1,2}$ are the two SU(2) Higgs doublets. This coupling is, therefore, generic to any version of a 2HDM.

The coupling $H^+ \bar{u}_i d_j$ is obtained from the Yukawa potential. The most general Yukawa interaction of a 2HDM can be written as (see e.g., [14]):

$$\begin{aligned} \mathcal{L}_Y &= - \sum_{i,j} \bar{Q}_L^i \left[\left(U_{ij}^1 \tilde{\Phi}_1 + U_{ij}^2 \tilde{\Phi}_2 \right) u_R^j \right. \\ &\quad \left. + \left(D_{ij}^1 \Phi_1 + D_{ij}^2 \Phi_2 \right) d_R^j \right], \end{aligned} \quad (23)$$

where Q_L is the SU(2) left-handed quark doublet, u_R and d_R are the right-handed up and down SU(2) singlets, respectively, and $\tilde{\Phi}_{1,2} = i\sigma_2 \Phi_{1,2}^*$. Also, U^1, U^2, D^1, D^2 are general Yukawa 3×3 matrices in flavor space. The different types of 2HDM's are then categorized according to the choice of the Yukawa matrices U^1, U^2, D^1, D^2 .

In what follows we will focus on two specific versions of a 2HDM:

• 2HDM of type II (2HDMII)

The 2HDMII follows from the choice $U^1 = 0$ and $D^2 = 0$ in which case only Φ_2 generates the masses of the up-type quarks and only Φ_1 is responsible for the mass generation of the down-type quarks [15]. This version of a 2HDM is realized in the Minimal Supersymmetric Standard Model (MSSM).

• 2HDM “for the top-quark” (T2HDM)

In the T2HDM [16], the large mass of the top-quark is accommodated in a natural fashion by coupling the second Higgs doublet (Φ_2), which has a much larger vacuum expectation value (VEV), only to the top-quark; all other quarks are coupled to the 1st Higgs doublet (Φ_1). This scenario is, therefore, realized by setting in (23):

$$U_{ij}^1 \rightarrow G_{ij} \times (\delta_{j1} + \delta_{j2}),$$

$$\begin{aligned} U_{ij}^2 &\rightarrow G_{ij} \times \delta_{j3}, \\ D_{ij}^2 &\rightarrow 0, \end{aligned} \quad (24)$$

where G is again an unknown Yukawa 3×3 matrix in quark flavor space.

Using the Lagrangian pieces given above, we list in Table I all the couplings required for the calculation of $\Gamma(Z \rightarrow d_I \bar{d}_J)$ in a 2HDMII and in a T2HDM. In Table I, s_W , c_W are the sine and cosine of the weak-mixing angle θ_W , $m_{u_i} = m_u$, m_c , m_t for $i = 1, 2, 3$, respectively, and

$$Y_{ij} = -\frac{e}{\sqrt{2}s_W} \frac{m_t}{M_W} \tan \beta V_{CKM}^{ij}. \quad (25)$$

with V_{CKM} the Cabibbo-Kobayashi-Maskawa (CKM) matrix and $\tan \beta \equiv t_\beta = v_2/v_1$ (we will loosely refer to the ratio v_2/v_1 either as $\tan \beta$ or t_β), where $v_2(v_1)$ is the VEV of $\Phi_2(\Phi_1)$. Also, the matrix Σ introduced in Table I is composed out of the unitary matrix that diagonalizes the right-handed up-type quarks and the Yukawa matrix U_{ij}^2 defined in (24). It, therefore, arises from the specific structure of the Yukawa interactions in the T2HDM and can be parametrized as follows [17] (neglecting the mass of the first generation up-quark):

$$\Sigma = \begin{pmatrix} 0 & 0 & 0 \\ 0 & m_c \varepsilon_{ct}^2 |\xi|^2 & m_c \varepsilon_{ct} \xi^* \\ 0 & m_c \xi \sqrt{1 - |\varepsilon_{ct} \xi|^2} & m_t (1 - |\varepsilon_{ct} \xi|^2) \end{pmatrix}, \quad (26)$$

where $\varepsilon_{ct} = m_c/m_t$ and ξ is an unknown parameter (assumed here to be real) whose “natural” size is of $\mathcal{O}(1)$.

Notice that the specific structure of the T2HDM’s Yukawa potential does not give rise to tree-level flavor changing couplings between a neutral Higgs and a pair of down-quarks (while allowing for tree-level neutral Higgs-top-charm couplings). Therefore, the decay $Z \rightarrow d_I \bar{d}_J$ is not affected at one-loop by flavor changing neutral Higgs-quark interactions.

A. $Z \rightarrow b\bar{s}$ in 2HDMII

The charged Higgs one-loop contribution to the decay $Z \rightarrow b\bar{s}$ in a 2HDMII was examined before in [4]. Here we wish to recapitulate the salient features of this decay.

On the left side of Fig. 2 we plot $BR(Z \rightarrow b\bar{s} + \bar{b}s)$ as a function of $\tan \beta$ for charged Higgs masses of 100, 400 and 600 GeV. As can be seen, $BR(Z \rightarrow b\bar{s} + \bar{b}s)$ is maximal for low $\tan \beta \sim \mathcal{O}(1)$ for which it is controlled by the top-quark Yukawa coupling which is $\propto 1/\tan \beta$. Thus, in this range the required flavor transition is mediated by $t \rightarrow s$ and the $BR(Z \rightarrow b\bar{s} + \bar{b}s)$ is, therefore, essentially proportional to $(m_t/\tan \beta)^4 \times (V_{CKM}^{tb})^2 (V_{CKM}^{ts})^2$ which is the square of the product of the tbH^+ and tsH^+ Yukawa couplings.

At around $\tan \beta \sim 13$ there is a “turning point” at which the $BR(Z \rightarrow b\bar{s} + \bar{b}s)$ starts to increase with $\tan \beta$. At this point the contributions from the top and charm-quark loop exchanges become comparable, since the charm-quark effect being $\propto m_s^2 m_b^2 \tan^4 \beta (V_{CKM}^{cs})^2 (V_{CKM}^{cb})^2$ (for $\tan \beta \gtrsim 13$ the charm-quark exchange is dominated by the Yukawa couplings b_R^{22} and b_R^{23} , see Table I) equals that of the top-quark. As $\tan \beta$ is further increased ($\tan \beta > 13$) both the top and charm-quark loop exchanges are dominated by the right-handed down-quark Yukawa couplings b_R^{ij} in (8) (which is $\propto \tan \beta$) and are, therefore, comparable and increasing with $\tan \beta$.

Note that the curves in Fig. 2 for the 2HDMII scenario (the left side) pass through unrealistic values in the $\tan \beta - m_{H^+}$ plane. In particular, the decay $b \rightarrow s\gamma$ imposes strong constraints on the $\tan \beta - m_{H^+}$ plane [18]: $m_{H^+} \gtrsim 400$ GeV independent of $\tan \beta$. Thus, if $\tan \beta = 1$, then the largest allowed value for the $BR(Z \rightarrow b\bar{s} + \bar{b}s)$ is $\sim 10^{-10}$ if m_{H^+} lies close to its lower bound from $b \rightarrow s\gamma$. For even smaller values of $\tan \beta$, say $\tan \beta \lesssim 0.5$, the $b \rightarrow s\gamma$ constraint requires $m_{H^+} \gtrsim 500$ GeV for which the $BR(Z \rightarrow b\bar{s} + \bar{b}s)$ is again $\lesssim 10^{-10}$ in the 2HDMII.

B. $Z \rightarrow b\bar{s}$ in T2HDM

The main difference between the T2HDM and the 2HDMII charged Higgs sectors lies in the structure of the $cd_i H^+$ Yukawa interactions ($d_i = d, s, b$ for $i = 1, 2, 3$ respectively). In particular, while in both models the top Yukawa coupling to down-quarks, i.e., the $\bar{t}_R d_L H^+$ coupling, is $\propto m_t V_{CKM}^{td}/\tan \beta$, the charm-quark Yukawa coupling is completely altered by the presence of the matrix Σ in (26). Specifically, the $\bar{c}_R b_L H^+$ coupling is $\propto m_c \xi^* V_{CKM}^{tb} \tan \beta$ and the $\bar{c}_R s_L H^+$ coupling is $\propto m_c V_{CKM}^{cs} \tan \beta$. These couplings are, therefore, a factor of $\tan^2 \beta \times (V_{CKM}^{tb}/V_{CKM}^{cb})$ and $\tan^2 \beta$, respectively, larger than in the 2HDMII if ξ is of $\mathcal{O}(1)$.

As can be seen from Fig. 2 (the right side), in the range $\tan \beta \lesssim 5$ the $BR(Z \rightarrow b\bar{s} + \bar{b}s)$ is practically identical in both the T2HDM and the 2HDMII; in this range it is dominated by the top-quark loop and, therefore, by the top-quark Yukawa couplings to the b and s -quarks which are essentially the same in these two versions of a 2HDM. On the other hand, for larger values of $\tan \beta$, in contrast to the case of a 2HDMII, in the T2HDM the charm-quark loop starts to dominate due to the enhancement in the $\bar{c}_R b_L H^+$ and $\bar{c}_R s_L H^+$ Yukawa couplings (see discussion above). In fact, the $\bar{c}_R b_L H^+$ coupling is doubly enhanced in the T2HDM; first by the $\tan \beta$ factor and second by a factor of $V_{CKM}^{tb}/V_{CKM}^{cb}$, i.e., in this model this coupling does not suffer from the CKM suppression factor V_{CKM}^{cb} .

It should be emphasized that a large $\tan \beta$, e.g., $\tan \beta \gtrsim \mathcal{O}(10)$, is the “working assumption” of the T2HDM. In particular, the T2HDM loses its attractiveness in the small $\tan \beta$ regime, since in this range it fails to explain the large top-quark mass - this being

	2HDMII	T2HDM
scalar ($S_{\alpha=1}$)	H^+	H^+
fermion (f_i)	$u_i, i = 1, 2, 3$	$u_i, i = 1, 2, 3$
$a_{L(Zf)}^{ij}$	$a_{L(Zu)}$	$a_{L(Zu)}$
$a_{R(Zf)}^{ij}$	$a_{R(Zu)}$	$a_{R(Zu)}$
$b_{L(\alpha=1)}^{ij}$	$Y_{ij} \times \frac{1}{\tan^2 \beta} \frac{m_{u_i}}{m_t}$	$Y_{ij} \times \left[\frac{\Sigma_{ik}^\dagger V_{ij}^{kj}}{m_t V_{ij}} \left(1 + \frac{1}{\tan^2 \beta} \right) - \frac{m_{u_i}}{m_t} \right]$
$b_{R(\alpha=1)}^{ij}$	$Y_{ij} \times \frac{m_{d_j}}{m_t}$	$Y_{ij} \times \frac{m_{d_j}}{m_t}$
$g_Z^{\alpha=1\beta=1}$	$-e \frac{1-2s_W^2}{2s_W c_W}$	$-e \frac{1-2s_W^2}{2s_W c_W}$

TABLE I: The couplings required for the calculation of $\Gamma(Z \rightarrow d_I \bar{d}_J)$ in a 2HDMII and a T2HDM. The couplings follow the notation used in the Feynman rules of (2), (7) and (8). Also, $a_{R(Zu)}$, $a_{L(Zu)}$ are given in (3)-(6).

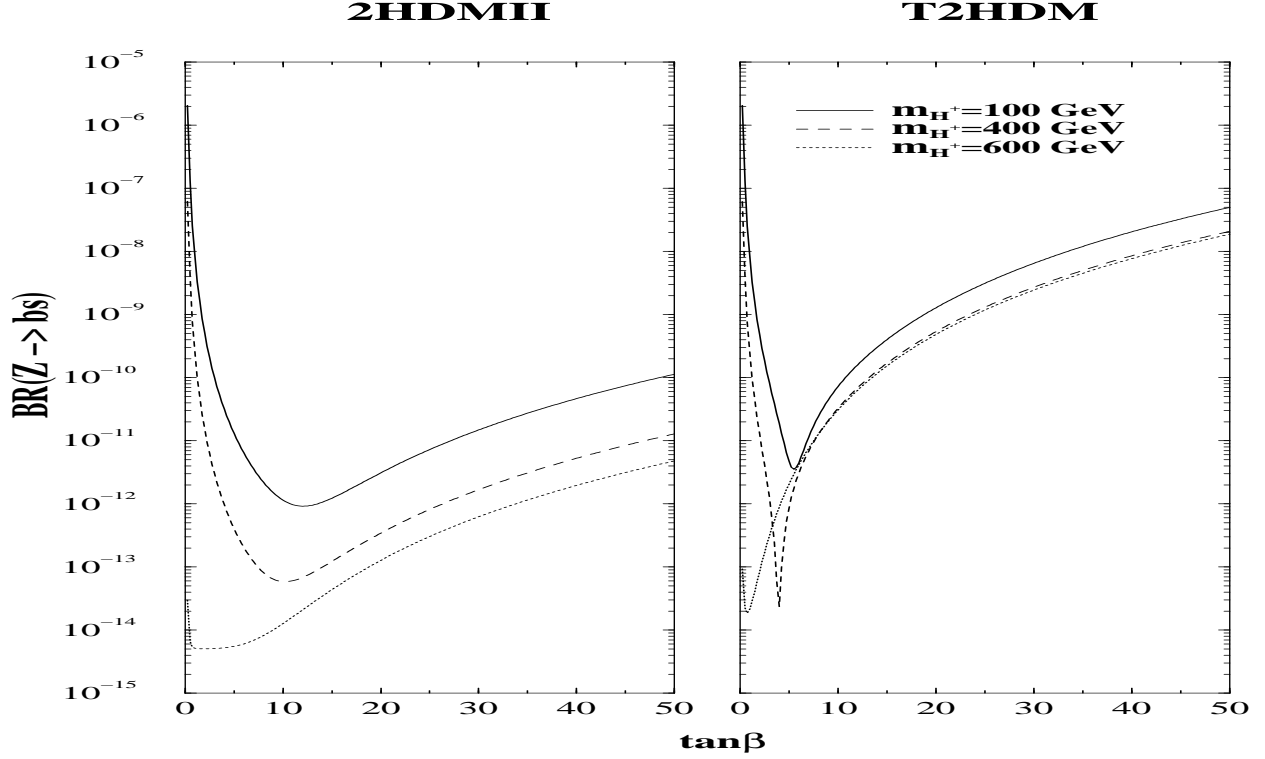


FIG. 2: $BR(Z \rightarrow b\bar{s} + \bar{b}s)$ as a function of $\tan \beta$, for $m_{H^+} = 100, 400$ and 600 GeV, in a 2HDMII (left side) and a T2HDM with $\xi = 1$ (right side).

the main motivation behind this version of a 2HDM. At the same time, taking into account low-energy experimental data from $K - \bar{K}$ mixing, ϵ_K and $b \rightarrow s\gamma$, the $\tan \beta - m_{H^+}$ plane is also constrained in the T2HDM [17, 19], especially in the large $\tan \beta$ region in which this model differs from the usual 2HDMII. For example, for $\xi = 1$ and taking the SM best fit value for the Wolfenstein parameters ρ and η , then the ϵ_K constraint implies

$m_{H^+} \gtrsim 500$ GeV for $\tan \beta \sim 20$ and $m_{H^+} \gtrsim 4$ TeV for $\tan \beta \sim 50$ [19]. Imposing these bounds we find that $BR(Z \rightarrow b\bar{s} + \bar{b}s) \sim \mathcal{O}(10^{-8})$ is the best case value in this model assuming a large $\tan \beta$.

IV. SUPERSYMMETRY WITH SQUARK MIXINGS

In SUSY flavor changing phenomena can emanate from mixings of squarks of different generations through the

$$\mathcal{L}_{soft}^{squark} = -\tilde{Q}_i^\dagger (M_Q^2)_{ij} \tilde{Q}_j - \tilde{U}_i^\dagger (M_U^2)_{ij} \tilde{U}_j - \tilde{D}_i^\dagger (M_D^2)_{ij} \tilde{D}_j + A_u^{ij} \tilde{Q}_i H_u \tilde{U}_j + A_d^{ij} \tilde{Q}_i H_d \tilde{D}_j , \quad (27)$$

where \tilde{Q} is the SU(2) scalar doublet and \tilde{U} , \tilde{D} are the up-squark, down-squark SU(2) singlets, respectively. Also, i, j are generation indices.

The mass matrices in the up-squark and down-squark sectors may then be generically expressed as:

$$M_{\tilde{U}, \tilde{D}}^2 = \begin{pmatrix} (m_{\tilde{U}, \tilde{D}}^2)_{LL} & (m_{\tilde{U}, \tilde{D}}^2)_{LR} \\ (m_{\tilde{U}, \tilde{D}}^2)_{LR}^\dagger & (m_{\tilde{U}, \tilde{D}}^2)_{RR} \end{pmatrix} \quad (28)$$

$$\begin{aligned} (m_{\tilde{U}}^2)_{LL} &\equiv V_L^U M_Q^2 V_L^{U\dagger} , & (m_{\tilde{D}}^2)_{LL} &\equiv V_L^D M_Q^2 V_L^{D\dagger} , \\ (m_{\tilde{U}}^2)_{RR} &\equiv V_R^U M_U^{2T} V_R^{U\dagger} , & (m_{\tilde{D}}^2)_{RR} &\equiv V_R^D M_D^{2T} V_R^{D\dagger} , \\ (m_{\tilde{U}}^2)_{LR} &\equiv -\frac{v \sin \beta}{\sqrt{2}} V_L^U A_u^* V_R^{U\dagger} , & (m_{\tilde{D}}^2)_{LR} &\equiv \frac{v \cos \beta}{\sqrt{2}} V_L^D A_d^* V_R^{D\dagger} , \end{aligned} \quad (29)$$

where $V_{L,R}^D$ and $V_{L,R}^U$ are the rotation matrices that diagonalize the down and up-quark fermion mass matrices, respectively (the CKM matrix is $V_{CKM} = V_L^U V_L^{D\dagger}$).

Assuming that flavor changing squark mixings are significant only in transitions between the third and second generation squarks, we choose the following textures for the 3×3 matrices $(m_{\tilde{U}, \tilde{D}}^2)_{LL}$ and $(m_{\tilde{U}, \tilde{D}}^2)_{RR}$:

$$(m_{\tilde{U}, \tilde{D}}^2)_{LL, RR} = \begin{pmatrix} 1 & 0 & 0 \\ 0 & 1 & \delta_{LL, RR}^{U, D(23)} \\ 0 & \delta_{LL, RR}^{U, D(32)} & 1 \end{pmatrix} m_0^2 , \quad (30)$$

where $\delta_{LL}^{U(23)}$, $\delta_{LL}^{U(32)}$, $\delta_{RR}^{U(23)}$, $\delta_{RR}^{U(32)}$ and $\delta_{LL}^{D(23)}$, $\delta_{LL}^{D(32)}$, $\delta_{RR}^{D(23)}$, $\delta_{RR}^{D(32)}$ represent flavor mixings in the $\tilde{t} - \tilde{c}$ and $\tilde{b} - \tilde{s}$ sectors, respectively. These flavor violating quantities emanate from non-diagonal entries in the bilinear soft breaking terms M_Q^2 , M_U^2 and M_D^2 in (27). Similarly, $\delta_{LR}^{U(23)}$, $\delta_{LR}^{U(32)}$ and $\delta_{LR}^{D(23)}$, $\delta_{LR}^{D(32)}$ are associated with non-diagonal (flavor changing) entries in the trilinear soft

soft breaking Lagrangian terms in the squark sector:

where $(m_{\tilde{U}, \tilde{D}}^2)_{LL}$, $(m_{\tilde{U}, \tilde{D}}^2)_{RR}$ and $(m_{\tilde{U}, \tilde{D}}^2)_{LR}$ are 3×3 matrices in squark flavor space. In the super CKM basis the squark fields are rotated “parallel” to their fermionic super-partners. In this basis, and assuming that there is a typical common mass scale for the squarks, m_0 , which is sufficiently heavier than the electroweak mass scale ($m_0^2/M_Z^2 \gg 1$), these matrices are related to the soft breaking bilinear and trilinear terms in (27) via [20]:

breaking terms A_u and A_d defined in (27). As in [21] we adopt the following simplified Ansatz:

$$V_L^U A_u^* V_R^{U\dagger} = \begin{pmatrix} 0 & 0 & 0 \\ 0 & 0 & x_u \\ 0 & y_u & 1 \end{pmatrix} A , \quad (31)$$

and

$$V_L^D A_d^* V_R^{D\dagger} = \begin{pmatrix} 0 & 0 & 0 \\ 0 & 0 & x_d \\ 0 & y_d & 1 \end{pmatrix} A , \quad (32)$$

such that A is a common trilinear soft breaking parameter for both up and down-squarks and the parameters x_u, y_u and x_d, y_d represent flavor mixing effects in the $\tilde{t} - \tilde{c}$ and $\tilde{b} - \tilde{s}$ sectors, respectively. It then follows that $\delta_{LR}^{U(23)}$, $\delta_{LR}^{U(32)}$ and $\delta_{LR}^{D(23)}$, $\delta_{LR}^{D(32)}$ are related to x_u , y_u and x_d , y_d via:

$$\delta_{LR}^{U(23)} = -x_u \frac{\sin \beta}{\sqrt{2}} \times \frac{vA}{m_0^2} , \quad \delta_{LR}^{U(32)} = -y_u \frac{\sin \beta}{\sqrt{2}} \times \frac{vA}{m_0^2} , \quad (33)$$

$$\delta_{LR}^{D(23)} = x_d \frac{\cos \beta}{\sqrt{2}} \times \frac{vA}{m_0^2}, \quad \delta_{LR}^{D(32)} = y_d \frac{\cos \beta}{\sqrt{2}} \times \frac{vA}{m_0^2}. \quad (34)$$

Within this mixing scenario, in which flavor changing effects in the squark sector are present only in the second and third generations, the 6×6 mass matrices in the up and down-squark sectors reduce to 4×4 matrices.

For the $\tilde{t}-\tilde{c}$ sector, in the basis $\Phi_U^0 = (\tilde{c}_L, \tilde{c}_R, \tilde{t}_L, \tilde{t}_R)$, we then have:

$$\tilde{M}_{ct}^2 = \begin{pmatrix} 1 & 0 & \delta_{LL}^{U(23)} & \delta_{LR}^{U(23)} \\ 0 & 1 & \delta_{LR}^{U(32)} & \delta_{RR}^{U(23)} \\ \delta_{LL}^{U(32)} & \delta_{LR}^{U(32)} & 1 & -X_t/m_0^2 \\ \delta_{LR}^{U(23)} & \delta_{RR}^{U(32)} & -X_t/m_0^2 & 1 \end{pmatrix} m_0^2, \quad (35)$$

and similarly for the $\tilde{b}-\tilde{s}$ sector, in the basis $\Phi_U^0 = (\tilde{s}_L, \tilde{s}_R, \tilde{b}_L, \tilde{b}_R)$, we have:

$$\tilde{M}_{sb}^2 = \begin{pmatrix} 1 & 0 & \delta_{LL}^{D(23)} & \delta_{LR}^{D(23)} \\ 0 & 1 & \delta_{LR}^{D(32)} & \delta_{RR}^{D(23)} \\ \delta_{LL}^{D(32)} & \delta_{LR}^{D(32)} & 1 & -X_b/m_0^2 \\ \delta_{LR}^{D(23)} & \delta_{RR}^{D(32)} & -X_b/m_0^2 & 1 \end{pmatrix} m_0^2. \quad (36)$$

The factors X_t and X_b are responsible for mixings between left and right handed squarks of the same generation and are given by:

$$X_t = \frac{v \sin \beta}{\sqrt{2}} A + \frac{m_t \mu}{\tan \beta}, \quad (37)$$

$$X_b = -\frac{v \cos \beta}{\sqrt{2}} A + m_b \tan \beta \mu, \quad (38)$$

where μ is the usual Higgs mass parameter in the SUSY superpotential.

After diagonalization of \tilde{M}_{ct}^2 and \tilde{M}_{sb}^2 one obtains the new mass-eigenstates which are now $\tilde{t}-\tilde{c}$ and $\tilde{b}-\tilde{s}$ admixtures, respectively. The diagonalizing matrices R_U and R_D are defined through:

$$\Phi_{U,i}^0 = R_{U,ik} \Phi_{U,k}, \quad \Phi_{D,i}^0 = R_{D,ik} \Phi_{D,k}, \quad (39)$$

where

$$\Phi_U^0 \equiv \begin{pmatrix} \tilde{c}_L \\ \tilde{c}_R \\ \tilde{t}_L \\ \tilde{t}_R \end{pmatrix}, \quad \Phi_U \equiv \begin{pmatrix} \tilde{c}_1 \\ \tilde{c}_2 \\ \tilde{t}_1 \\ \tilde{t}_2 \end{pmatrix}, \quad \Phi_D^0 \equiv \begin{pmatrix} \tilde{s}_L \\ \tilde{s}_R \\ \tilde{b}_L \\ \tilde{b}_R \end{pmatrix}, \quad \Phi_D \equiv \begin{pmatrix} \tilde{s}_1 \\ \tilde{s}_2 \\ \tilde{b}_1 \\ \tilde{b}_2 \end{pmatrix}, \quad (40)$$

and $\tilde{u}_{L,R}$, $\tilde{d}_{L,R}$ ($u = c, t$ and $d = s, b$) are the SU(2) weak states, while $\tilde{u}_{1,2}$, $\tilde{d}_{1,2}$ are the corresponding physical states (mass-eigenstates).

Let us now consider separately the cases in which the one-loop flavor changing decay $Z \rightarrow b\bar{s}$ is driven either by the $\tilde{t}-\tilde{c}$ or by the $\tilde{b}-\tilde{s}$ mixing phenomena.

A. $\tilde{b}-\tilde{s}$ mixing

Here the flavor changing decay $Z \rightarrow b\bar{s}$ is generated by one-loop exchanges of the $\tilde{b}-\tilde{s}$ admixture states, Φ_D , and gluinos, \tilde{g} . We thus have $S_\alpha = \Phi_{D,\alpha}$ with $\alpha = 1-4$, and $f = \tilde{g}$ in the diagrams of Fig. 1. Note that diagram (2) in Fig. 1, which requires the Vff coupling, does not contribute since the Z -boson does not couple to gluinos at tree-level.

The one-loop $\tilde{b}-\tilde{s}$ mixing effect on the decay $Z \rightarrow b\bar{s}$ was considered more than a decade ago in [5], where it

was assumed that flavor violation in the down-squark sector is controlled by radiative corrections to the down-squark mass matrix induced by off-diagonal CKM elements. Instead, as described above, we assume here that the flavor violation is rooted with non-diagonal entries in the soft SUSY breaking sector. The approach taken here is, therefore, fundamentally different from the one suggested in [5].^[1]

The following interaction vertices are required for the calculation of $\Gamma(Z \rightarrow b\bar{s})$ in the $\tilde{b}-\tilde{s}$ mixing scenario:

$$V_\mu S_\alpha S_\beta \rightarrow Z_\mu \Phi_{D,\alpha}^* \Phi_{D,\beta}, \quad (41)$$

$$S_\alpha \tilde{f}_i d_j \rightarrow \Phi_{D,\alpha}^* \tilde{g} d_j.$$

These are derived from [22]:

[1] Note also that [5] used unrealistic top-quark and squark masses.

$$\begin{aligned} \mathcal{L}(V_\mu \tilde{d} \tilde{d}) = & -i \left[-\frac{1}{2} \frac{e}{s_W} A_\mu^3 + \frac{1}{6} \frac{e}{c_W} B_\mu \right] \tilde{d}_{L,\ell}^* \overleftrightarrow{\partial}_d^\mu \tilde{d}_{L,\ell} \\ & -i \frac{1}{3} \frac{e}{c_W} B_\mu \tilde{d}_{R,\ell}^* \overleftrightarrow{\partial}_d^\mu \tilde{d}_{R,\ell}^* , \end{aligned} \quad (42)$$

$$\mathcal{L}(\tilde{d} \tilde{g} d) = g_s \sqrt{2} T^a \tilde{g} \left(-\tilde{d}_{L,\ell}^* L + \tilde{d}_{R,\ell}^* R \right) d_j + h.c. , \quad (43)$$

where g_s is the SU(3) coupling constant and T^a are the SU(3) group generators.

Using the above interaction Lagrangian terms, the couplings required for the calculation of $\Gamma(Z \rightarrow b\bar{s})$ in the form defined in (7) and (8) are obtained by rotating the weak states, Φ_D^0 , to the physical states, Φ_D , according to (39). These couplings are given in Table II.

	SUSY with $\tilde{b} - \tilde{s}$ mixing
scalar (S_α)	$\Phi_{D,\alpha}, \quad \alpha = 1, 2, 3, 4$
fermion (f_i)	\tilde{g}
$a_{L(Zf)}^{ij}$	0
$a_{R(Zf)}^{ij}$	0
$b_{L(\alpha)}^{ij}$	$-\sqrt{2} g_s T^a (R_{D,3\alpha}^* \delta_{3j} + R_{D,1\alpha}^* \delta_{2j})$
$b_{R(\alpha)}^{ij}$	$-\sqrt{2} g_s T^a (R_{D,4\alpha}^* \delta_{3j} + R_{D,2\alpha}^* \delta_{2j})$
$g_Z^{\alpha\beta}$	$\frac{-e}{2s_W c_W} (R_{D,1\alpha}^* R_{D,1\beta} + R_{D,3\alpha}^* R_{D,3\beta} - \frac{2}{3} s_W^2 \delta_{\alpha\beta})$

TABLE II: The couplings required for the calculation of $\Gamma(Z \rightarrow b\bar{s})$ in the MSSM with $\tilde{b} - \tilde{s}$ mixing. These couplings follow the notation used in the Feynman rules defined by (2), (7) and (8).

The relevant low-energy SUSY parameter space for the $\tilde{b} - \tilde{s}$ mixing scenario is characterized as follows:[2]

- I. Some of the flavor changing parameters in the $\tilde{b} - \tilde{s}$ sector are severely constrained by the $b \rightarrow s\gamma$ decay [20, 23]. In particular, $\delta_{LR}^{D(23)}, \delta_{LR}^{D(32)} \lesssim \mathcal{O}(10^{-2})$ is required in order to keep $BR(b \rightarrow s\gamma)$ within its experimental measured value.[3] On the other hand,

$\delta_{LL}^{D(23)}, \delta_{LL}^{D(32)}, \delta_{RR}^{D(23)}$ and $\delta_{RR}^{D(32)}$ of $\mathcal{O}(1)$ are not ruled out by $b \rightarrow s\gamma$ nor by any other low energy process that we know of.

We will, thus, use the LL and RR delta's as the only source for $\tilde{b} - \tilde{s}$ mixing. Moreover, since there is no a-priori theoretical reason for the four LL and RR delta's to be significantly different, we will set all of them to a common value denoted by δ^D . That is, we fix $\delta_{LL}^{D(23)} = \delta_{LL}^{D(32)} = \delta_{RR}^{D(23)} = \delta_{RR}^{D(32)} = \delta^D$, and vary δ^D in the range $0 < \delta^D < 1$.

- II. The SUSY parameter space needed to evaluate $\Gamma(Z \rightarrow b\bar{s})$ in this scenario is: $m_0, \mu, A, \tan\beta, m_{\tilde{g}}$ and δ^D . The low-energy values of these six parameters fully determine the $\tilde{b} - \tilde{s}$ scalar spectrum (i.e., masses and mixing matrices) and the gluino mass ($m_{\tilde{g}}$), from which all the couplings in Table II are calculated. These six parameters will be varied subject to the requirement that squark masses as well as the gluino mass are heavier than 150 GeV.

In Figs. 3, 5 and 7 we plot $BR(Z \rightarrow b\bar{s} + \bar{b}s)$ as a function μ, δ^D and $\tan\beta$, respectively, for three values of the common squark mass: $m_0 = 1000, 1600$ or 2200 GeV. The rest of the parameters are varied subject to the above criteria [24]. In order to better understand the dependence of $BR(Z \rightarrow b\bar{s} + \bar{b}s)$ on the physical squark mass spectrum, we accompany Figs. 3 and 5 by Figs. 4 and 6, respectively, in which we depict the masses of the four physical squarks $m_{\tilde{s}_{1,2}}$ and $m_{\tilde{b}_{1,2}}$ that correspond to the same choices of the SUSY parameter space as in Figs. 3 and 5.

Let us summarize the results shown in Figs. 3-7:

- The branching ratio of the decay $Z \rightarrow b\bar{s}$ is enhanced dramatically with the increase of the mass splittings between the four physical squarks. This is due to a GIM-like cancellation which is operational in the limit of degenerate squark masses as a result of the unitarity of the rotation matrix R_D .^[4] Thus for example, a typical mass spectrum that can drive the branching ratio to the 10^{-6} level is when the lightest down squark, \tilde{b}_1 , has a mass below 250 GeV, while the rest of the squarks have masses at the 1-3 TeV range.
- As expected, $BR(Z \rightarrow b\bar{s})$ drops sharply as δ^D is decreased. Clearly, this is traced to the fact that the mixing among the bottom and strange type scalars diminishes in the limit $\delta^D \rightarrow 0$, see Figs. 5 and 6.

[2] The term “low-energy” refers to the electroweak (or collider energies) scale and is used in order to distinguish it from the scale in which the soft breaking couplings are generated (e.g., the GUT scale).

[3] The bounds on the different delta's reported in [20, 23] were obtained using the mass insertion approximation, while we perform an exact diagonalization of the squark mass matrices. There-

fore, in the cases where $\mathcal{O}(1)$ delta's are allowed (e.g., for $\delta_{LL}^{D(32)}$) these bounds may only serve as indicative for their expected size, since the mass insertion approximation necessarily assumes small delta's.

[4] The unitarity of R_D also ensures that the infinities that appear in the individual diagrams of Fig. 1 cancel.

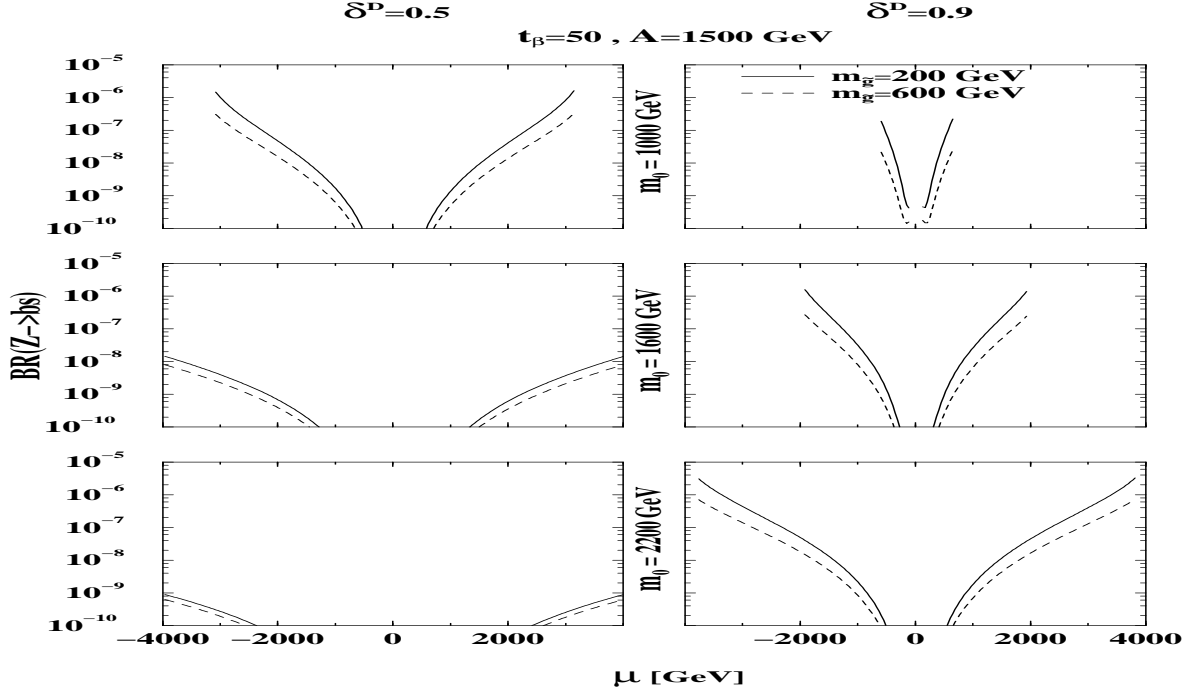


FIG. 3: $BR(Z \rightarrow b\bar{s} + \bar{b}s)$ as a function of the Higgs mass parameter μ , for combinations of $m_0 = 1000, 1600, 2200$ GeV with $m_{\tilde{g}} = 200, 600$ GeV, for $t_\beta = 50$, $A = 1500$ GeV and for $\delta^D = 0.5$ (left plots) and $\delta^D = 0.9$ (right plots).

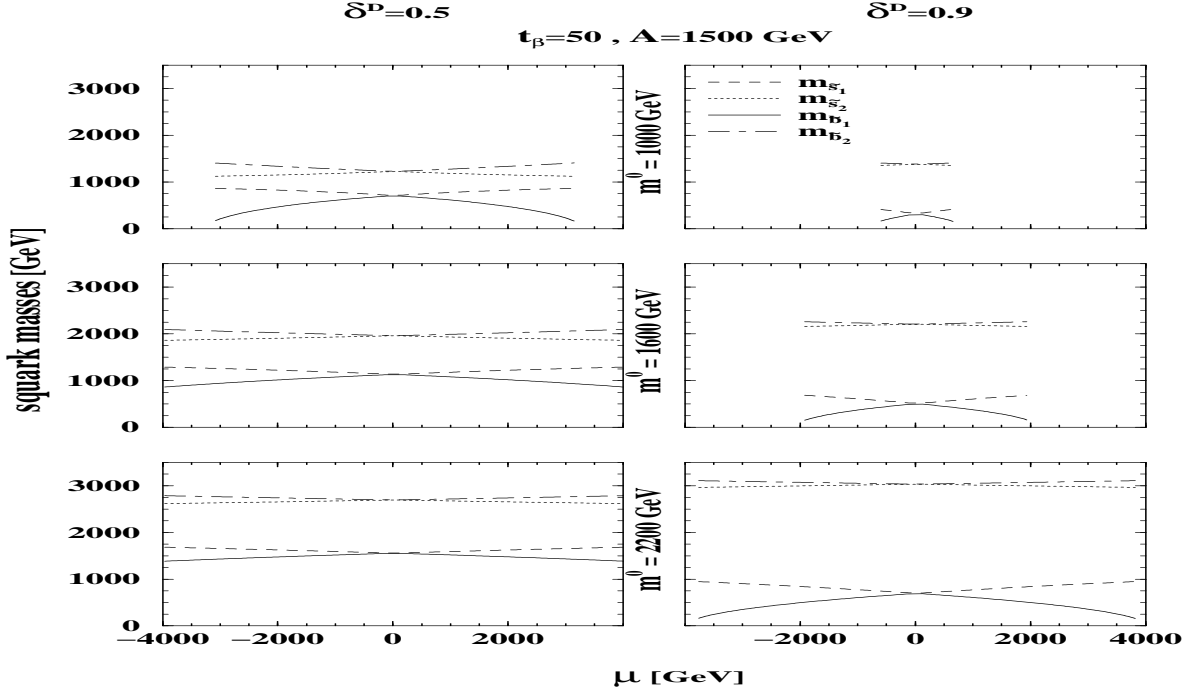


FIG. 4: Physical masses of the second and third generation down-type squarks as a function μ . The rest of the parameters are as in Fig. 3.

- For a sufficiently large $\tan\beta$, $BR(Z \rightarrow b\bar{s})$ is almost insensitive to the value of the common trilinear soft breaking parameter A as long as μ is large enough to drive the desired mass splittings between the squarks. This behavior is due to the dominance

of the μ term in the quantity X_b defined in (38) for large t_β (recall that X_b is responsible for the mass splitting between the two bottom-type scalars). On the other hand, for $t_\beta \sim \mathcal{O}(1)$, the term $\propto A$ in X_b (see the r.h.s. of (38)) becomes important when

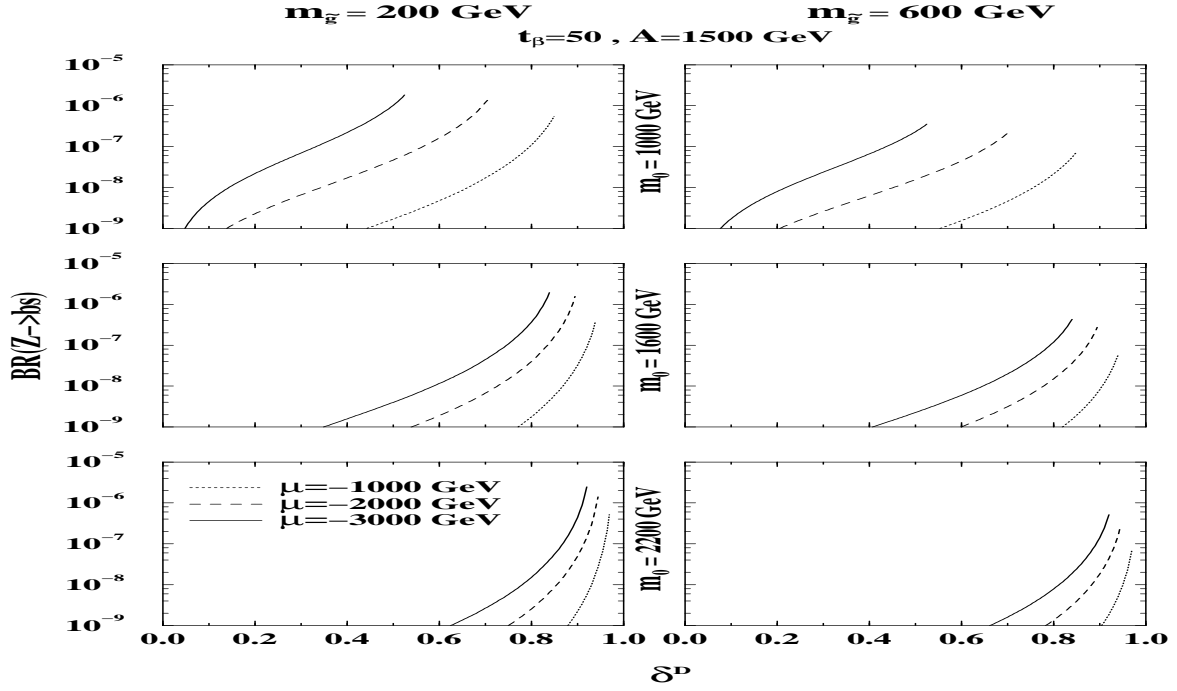


FIG. 5: $BR(Z \rightarrow b\bar{s} + \bar{b}s)$ as a function of the flavor mixing parameter δ^D , for combinations of $m_0 = 1000, 1600, 2200$ GeV with $\mu = -1000, -2000, -3000$ GeV, for $t_\beta = 50$, $A = 1500$ GeV and for $m_{\tilde{g}} = 200$ GeV (left plots) and $m_{\tilde{g}} = 600$ GeV (right plots).

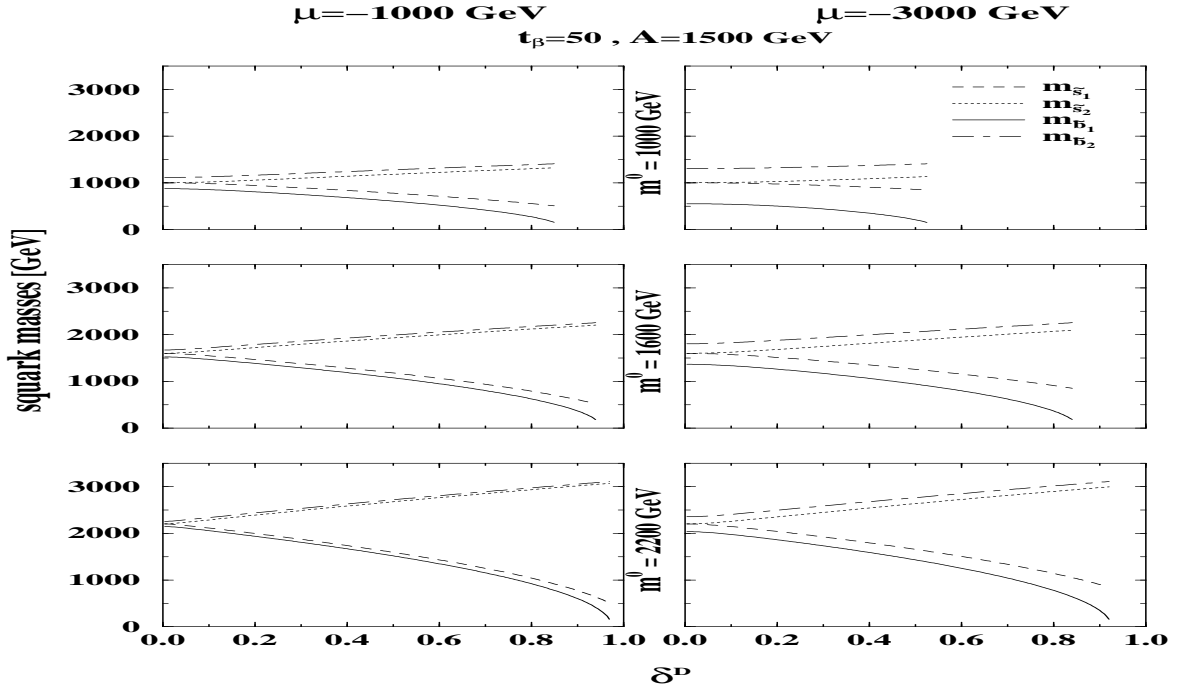


FIG. 6: Physical masses of the second and third generation down-type squarks, as a function of δ^D , for $m_0 = 1000, 1600, 2200$ GeV with $\mu = -1000$ GeV (left plots) and $\mu = -3000$ GeV (right plots). The rest of the parameters are as in Fig. 5.

$A \sim \mu$. This feature can be seen in Fig. 7.

- For the reason outlined above, $BR(Z \rightarrow b\bar{s})$ is symmetric about $\mu = 0$ for large $\tan\beta$, in which case the term $\propto \mu$ in X_b dominates and the effect of the

A term is negligible.

- For $\mu^2/A^2 \gg 1$, $BR(Z \rightarrow b\bar{s})$ is increased with $\tan\beta$. Again, this is related to the dominance of the μ term in X_b for large $\tan\beta$.

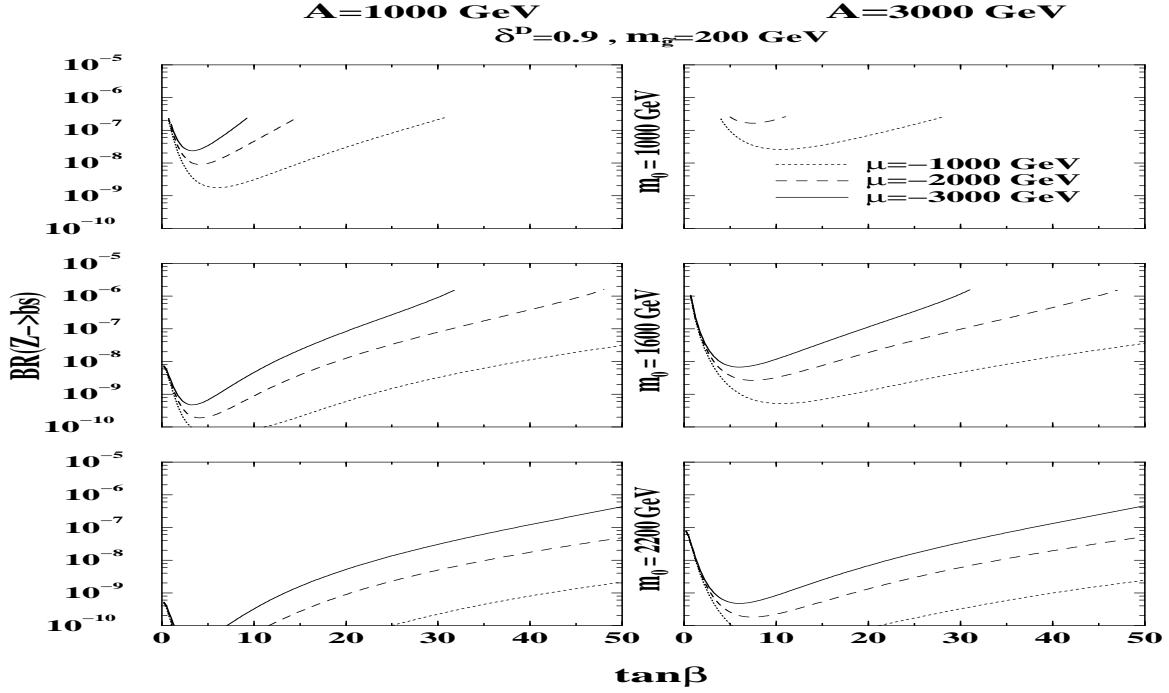


FIG. 7: $BR(Z \rightarrow b\bar{s} + \bar{b}s)$ as a function of $\tan\beta$, for combinations of $m_0 = 1000, 1600, 2200$ GeV with $\mu = -1000, -2000, -3000$ GeV, for $m_{\tilde{g}} = 200$ GeV, $\delta^D = 0.9$ GeV and for $A = 1000$ GeV (left plots) and $A = 3000$ GeV (right plots).

- $BR(Z \rightarrow b\bar{s})$ drops with $m_{\tilde{g}}$.

To conclude this section, we have shown that $BR(Z \rightarrow b\bar{s}) \sim \mathcal{O}(10^{-6})$ can be achieved in the $\tilde{b} - \tilde{s}$ mixing scenario provided that the gluino mass and one of the third generation down-type scalar masses lie close to the electroweak mass scale, while the rest of the down-type squark masses are at the TeV range, i.e., a large mass splitting between the lightest and rest of the down-type squarks is needed. Such a mass hierarchy in the squark sector requires a typical “heavy” SUSY mass scale with soft breaking parameters at the level of a few TeV. This scenario is somewhat motivated by the non-observability of SUSY particles in past and present high energy colliders.

B. $\tilde{t} - \tilde{c}$ mixing

In the stop-scharm mixing scenario the flavor changing decay $Z \rightarrow b\bar{s}$ proceeds through one-loop exchanges of

the $\tilde{t} - \tilde{c}$ admixture states, Φ_U , and charginos, χ . More specifically, we have $S_\alpha = \Phi_{U,\alpha}$ with $\alpha = 1 - 4$, and $f_i = \chi_i^c$ with $i = 1, 2$ for the two charginos (we find it convenient to calculate the exchanges of the charged conjugate chargino states χ^c).

Thus, in the $\tilde{t} - \tilde{c}$ mixing scenario the following interaction vertices are required:

$$\begin{aligned} V_\mu f_i \bar{f}_j &\rightarrow Z_\mu \chi_i^c \bar{\chi}_j^c, \\ V_\mu S_\alpha S_\beta &\rightarrow Z_\mu \Phi_{U,\alpha}^* \Phi_{U,\beta}, \\ S_\alpha \bar{f}_i d_j &\rightarrow \Phi_{U,\alpha}^* \bar{\chi}_i^c d_j. \end{aligned} \quad (44)$$

These vertices are taken from [22]:

$$\mathcal{L}(V_\mu \chi_i^c \bar{\chi}_j^c) = -\frac{e}{2s_W c_W} \bar{\chi}_j^c \gamma_\mu \left(a_{L(V\chi^c)}^{ij} L + a_{R(V\chi^c)}^{ij} R \right) \chi_i^c V_\mu, \quad (45)$$

$$\mathcal{L}(V_\mu \tilde{u} \tilde{u}) = -i \left[\frac{1}{2} \frac{e}{s_W} A_\mu^3 + \frac{1}{6} \frac{e}{c_W} B_\mu \right] \tilde{u}_{L,\ell}^* \overset{\leftrightarrow}{\partial}_u^\mu \tilde{u}_{L,\ell} + i \frac{2}{3} \frac{e}{c_W} B_\mu \tilde{u}_{R,\ell} \overset{\leftrightarrow}{\partial}_u^\mu \tilde{u}_{R,\ell}^*, \quad (46)$$

$$\mathcal{L}(\tilde{u} \chi^c d) = \tilde{u}_{L,\ell} \bar{d}_j \left(f_L^{L(\ell ij)} L + f_L^{R(\ell ij)} R \right) \chi_i^c V_{CKM}^{\ell j*} + \tilde{u}_{R,\ell} \bar{d}_j \left(f_R^{L(\ell ij)} L + f_R^{R(\ell ij)} R \right) \chi_i^c V_{CKM}^{\ell j*} + h.c., \quad (47)$$

where

$$a_{L(Z\chi^c)}^{ij} = (Z_{1i}^- Z_{1j}^{*-} + \cos 2\theta_W \delta_{ij}) , \quad (48)$$

	SUSY with $\tilde{t} - \tilde{c}$ mixing
scalar (S_α)	$\Phi_{U,\alpha}, \quad \alpha = 1, 2, 3, 4$
fermion (f_i)	$\chi_i^c, \quad i = 1, 2$
$a_{L(Zf)}^{ij}$	$-\frac{e}{2s_W c_W} a_{L(Z\chi^c)}^{ij}$
$a_{R(Zf)}^{ij}$	$-\frac{e}{2s_W c_W} a_{R(Z\chi^c)}^{ij}$
$b_{L(\alpha)}^{ij}$	$f_L^{R(\alpha ij)*} (R_{U,1\alpha}^* V_{CKM}^{2j} + R_{U,3\alpha}^* V_{CKM}^{3j}) + \frac{f_R^{R(\alpha ij)*}}{m_{u\alpha}} (m_c R_{U,2\alpha}^* V_{CKM}^{2j} + m_t R_{U,4\alpha}^* V_{CKM}^{3j})$
$b_{R(\alpha)}^{ij}$	$f_L^{L(\alpha ij)*} (R_{U,1\alpha}^* V_{CKM}^{2j} + R_{U,3\alpha}^* V_{CKM}^{3j})$
$g_Z^{\alpha\beta}$	$\frac{e}{2s_W c_W} (R_{U,1\alpha}^* R_{U,1\beta} + R_{U,3\alpha}^* R_{U,3\beta} - \frac{4}{3} s_W^2 \delta_{\alpha\beta})$

TABLE III: The couplings required for the calculation of $\Gamma(Z \rightarrow b\bar{s})$ in the $\tilde{t} - \tilde{c}$ mixing scenario. The couplings follow the notation in (2), (7) and (8). Also, $a_{L(Z\chi^c)}^{ij}$ and $a_{R(Z\chi^c)}^{ij}$ are given in (48) and (49), $f_L^{R(\alpha ij)*}$, $f_R^{R(\alpha ij)*}$ and $f_L^{L(\alpha ij)*}$ are defined in (50). R_U is the rotation matrix defined in (39).

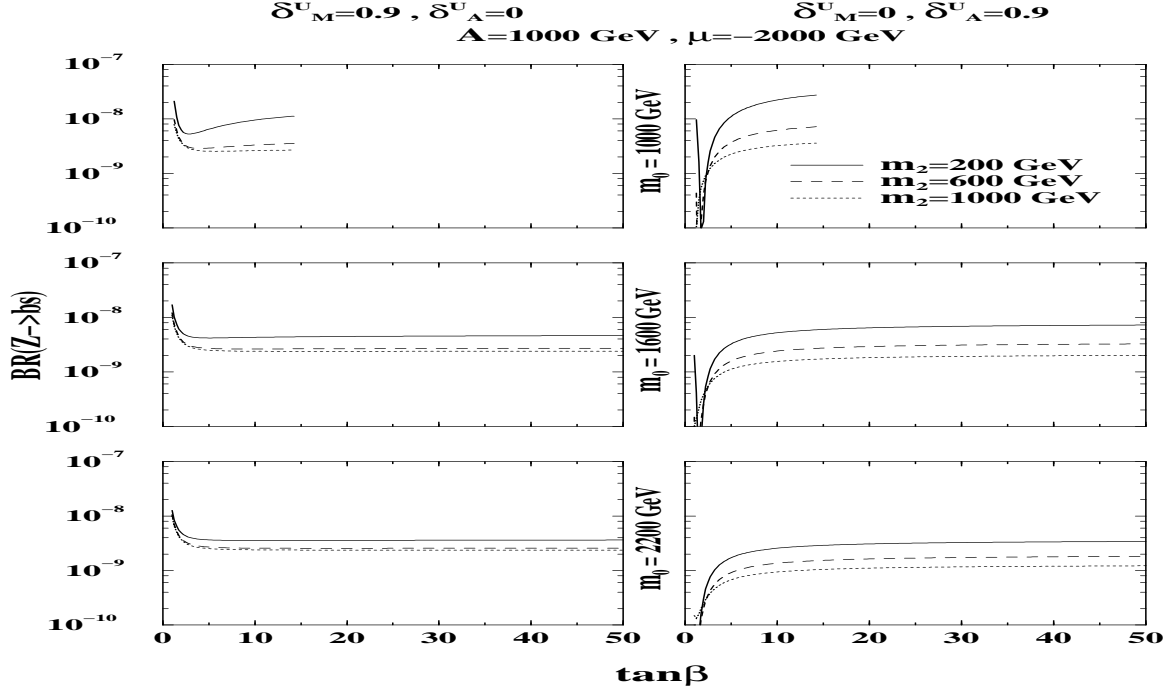


FIG. 8: $BR(Z \rightarrow b\bar{s} + \bar{b}s)$ as a function of $\tan\beta$, for combinations of $m_0 = 1000, 1600, 2200$ GeV with $m_2 = 200, 600, 1000$ GeV, for $A = 1000$ GeV, $\mu = -2000$ GeV and for $\delta_M^U = 0.9, \delta_A^U = 0$ (left plots) and $\delta_M^U = 0, \delta_A^U = 0.9$ (right plots).

$$a_{R(Z\chi^c)}^{ij} = (Z_{1i}^{+\star} Z_{1j}^+ + \cos 2\theta_W \delta_{ij}) , \quad (49)$$

$$f_L^{L(\ell ij)} = \frac{e}{\sqrt{2}s_W} \frac{m_{d_j}}{M_W \cos \beta} Z_{2i}^- ,$$

$$f_L^{R(\ell ij)} = -\frac{e}{s_W} Z_{1i}^{+\star} ,$$

$$f_R^{L(\ell ij)} = 0 ,$$

$$f_R^{R(\ell ij)} = \frac{e}{\sqrt{2}s_W} \frac{m_{u_\ell}}{M_W \sin \beta} Z_{2i}^{+\star} . \quad (50)$$

and Z^\pm are the chargino mixing matrices given in [22]. Also, A^3 and B are the SU(2) and U(1) gauge fields, respectively, and $\tilde{u}_{L,R}$ are the SU(2) weak states of the

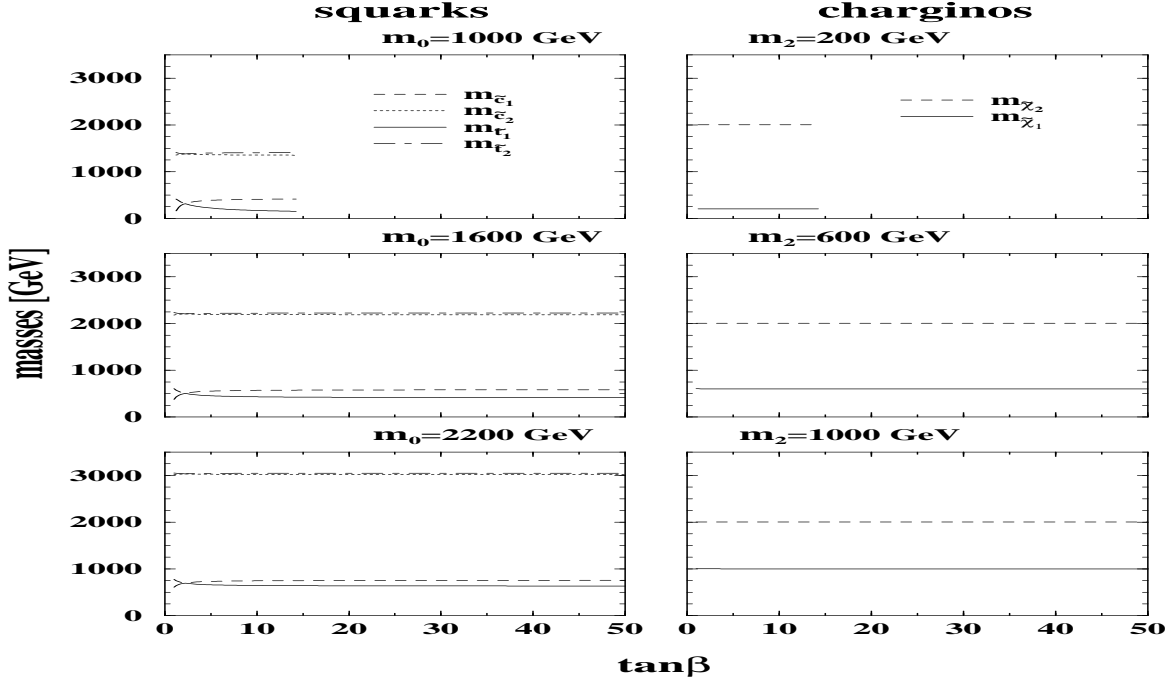


FIG. 9: Physical masses of the second and third generation up-type squarks (left plots) and of the charginos (right plots), as a function of $\tan\beta$. Squark masses are shown for $m_0 = 1000, 1600$ and 2200 GeV and for $\delta_M^U = 0.9, \delta_A^U = 0$ (equivalent to the case $\delta_M^U = 0, \delta_A^U = 0.9$, see text) and chargino masses are given for $m_2 = 200, 600$ and 1000 GeV. The rest of the parameters are as in Fig. 8.

up-type scalars.

Here also, the couplings needed for the calculation of $\Gamma(Z \rightarrow b\bar{s})$ in the form defined in (2), (7) and (8) are obtained from the Lagrangian terms in (45)-(50) by rotating the weak states, Φ_U^0 , to the physical states, Φ_U , according to (39). These couplings are summarized in Table III.

The contribution of the $\tilde{t} - \tilde{c}$ mixed states to the one-loop diagrams in Fig. 1 are characterized as follows:

- I. The quantities that mediate the flavor changing transition $b \rightarrow s$ in the $\tilde{t} - \tilde{c}$ mixed scenario are: $\delta_{LL}^{U(23)}, \delta_{LL}^{U(32)}, \delta_{RR}^{U(23)}, \delta_{RR}^{U(32)}, \delta_{LR}^{U(23)}$ and $\delta_{LR}^{U(32)}$. Recall that the LL and RR delta's originate from the bilinear soft terms in (27), while the LR delta's are associated with the trilinear soft breaking SUSY terms. Thus, we will separate these two types of flavor violating sources in our numerical analysis. In particular, we define $\delta_M^U = \delta_{LL}^{U(23)} = \delta_{LL}^{U(32)} = \delta_{RR}^{U(23)} = \delta_{RR}^{U(32)}$ and $\delta_A^U = \delta_{LR}^{U(23)} = \delta_{LR}^{U(32)}$ and we vary either δ_M^U or δ_A^U in the range $[0, 1]$. Note that an $\mathcal{O}(1)$ value for either δ_M^U or δ_A^U is consistent with all experimental data [20, 23].
- II. The required SUSY parameter space is: $m_0, \mu, A, \tan\beta, m_2$ and δ_M^U, δ_A^U , where m_2 is the SU(2) gaugino mass parameter. The low-energy values of these six parameters fix the $\tilde{t} - \tilde{c}$ scalar spectrum (i.e., masses and mixing matrices) and the chargino masses and mixing

matrices from which all couplings in Table III are derived.

As in the $\tilde{b} - \tilde{s}$ mixing case, these parameters will be varied subject to the requirement that the squark masses are heavier than 150 GeV and, in addition, that the charginos are heavier than 100 GeV [24].

Taking maximal flavor violation in the $\tilde{t} - \tilde{c}$ mixing scenario, i.e., $\delta_M^U \sim \mathcal{O}(1)$ or $\delta_A^U \sim \mathcal{O}(1)$, and varying the rest of the SUSY parameters involved subject to the above criteria, we find that $BR(Z \rightarrow b\bar{s} + \bar{b}s)$ can reach $\text{few} \times 10^{-8}$ at best. Here also, the $BR(Z \rightarrow b\bar{s} + \bar{b}s)$ is significantly enhanced when large mass splittings between the four up-type squarks, $m_{\tilde{c}_{1,2}}$ and $m_{\tilde{t}_{1,2}}$ are present. Such a hierarchy in the up-type squark mass spectrum makes the GIM-like cancellation mentioned earlier less effective.

Indeed a two orders of magnitude difference between the $\tilde{t} - \tilde{c}$ and $\tilde{b} - \tilde{s}$ mixing cases is expected due to an $(\alpha_s/\alpha)^2$ enhancement factor in the $\tilde{b} - \tilde{s}$ scenario (compared to the $\tilde{t} - \tilde{c}$ mixing case) which arises from the gluino QCD coupling.

In Figs. 8 we plot $BR(Z \rightarrow b\bar{s} + \bar{b}s)$ as a function of $\tan\beta$, for combinations of $m_0 = 1000, 1600$ and 2200 GeV with $m_2 = 200, 600$ and 1000 GeV and for either $\{\delta_M^U = 0.9, \delta_A^U = 0\}$ or $\{\delta_M^U = 0, \delta_A^U = 0.9\}$.^[5] For illus-

[5] Note that the physical up-squark masses have the same dependence on δ_M^U or δ_A^U when one of the two delta's is set to zero.

tration we set $A = 1000$ GeV and $\mu = -2000$ GeV. In Figs. 9 we depict the masses of the four physical up-type squarks $m_{\tilde{c}_{1,2}}$ and $m_{\tilde{t}_{1,2}}$ and the masses of the two chargino states as a function of $\tan \beta$, for the same SUSY parameter choices as in Figs. 8 [24].

V. SUSY WITH R_P VIOLATING INTERACTIONS

If R_P is violated in the SUSY superpotential, then flavor changing transitions can emerge from interactions of squarks or sleptons with fermions. In particular, there are two types of RPV terms that are allowed in the superpotential if the discrete R_P symmetry is not imposed. These are the RPV trilinear Yukawa-like (RPVT) operators and bilinear (RPVB) operators.

In the usual convention, the RPVT are proportional to the dimensionless couplings λ , λ' and λ'' , see e.g., [25]. Here we will assume that $\lambda'' \ll \lambda'$ and investigate the one-loop effects of the λ' type operator on our flavor changing decay $Z \rightarrow d_I \bar{d}_J$.^[6]

$$\mathcal{W}_{RPVT} \supset \epsilon_{ab} \lambda'_{ijk} \hat{L}_i^a \hat{Q}_j^b \hat{D}_k^c, \quad (51)$$

where \hat{Q} and \hat{L} are SU(2) doublet quark and lepton supermultiplets, respectively, and \hat{D} is the SU(2) singlet down-type quark supermultiplet. Also, $i, j, k = 1, 2$ or 3 are generation indices and a, b are SU(2) indices.

The RPVB operator is:

$$\mathcal{W}_{RPVB} = -\epsilon_{ab} \mu_i \hat{L}_i^a \hat{H}_u^b, \quad (52)$$

where \hat{H}_u is the up-type Higgs supermultiplet and $i = 1, 2$ or 3 labels the lepton generation.

In addition, if one does not impose R_P , then the usual set of R_P conserving (RPC) soft SUSY breaking terms is extended by new trilinear and bilinear soft terms which correspond to the RPV terms of the superpotential, i.e., to the ones in (51) and (52). For our purpose, only the following soft SUSY breaking bilinear term is relevant [26, 27, 28]:

$$V_{RPVB} = \epsilon_{ab} b_i \tilde{L}_i^a H_u^b, \quad (53)$$

where \tilde{L} and H_u are the scalar components of \hat{L} and \hat{H}_u , respectively.

The RPVT operator ($\propto \lambda'$) in (51) gives rise to the following scalar-fermion-fermion RPV interactions:

$$\begin{aligned} \mathcal{L} = & \lambda'_{ijk} \left\{ \tilde{\nu}_L^i \bar{d}_R^k d_L^j + \tilde{d}_L^j \bar{d}_R^k \nu_L^i + \left(\bar{d}_R^k \right)^* (\bar{\nu}_L^i)^c d_L^j \right. \\ & \left. - \tilde{e}_L^i \bar{d}_R^k u_L^j - \tilde{u}_L^j \bar{d}_R^k e_L^i - \left(\bar{d}_R^k \right)^* (\bar{e}_L^i)^c u_L^j \right\} + h.c. . \quad (54) \end{aligned}$$

where $d(u)$ is a down(up)-quark, $e(\nu)$ is a charged-lepton(neutrino) and scalars are denoted with a tilde.

The RPVB operator ($\propto \mu_i$) in (52) gives rise to mixings among charged leptons and charginos as well as between neutrinos and neutralinos. However, low energy flavor changing processes [29], flavor changing leptonic Z-decays [30] and neutrino masses [26, 30, 31, 32] suggest that the μ_i are expected to be vanishingly small. We will, therefore, neglect its contribution to the decay $Z \rightarrow d_I \bar{d}_J$.^[7] On the other hand, the soft breaking RPVB term ($\propto b_i$) in (53) gives rise to mixings between sleptons and Higgs-bosons which may be exchanged in the loops of the diagrams shown in Fig.1.

Let us now categorize the different types of RPV interactions that contribute at one-loop to the flavor changing decay of $Z \rightarrow d_I \bar{d}_J$. Since the decay $Z \rightarrow d_I \bar{d}_J$ conserves R_P , there should be two insertions of RPV vertices in the one-loop diagrams of Fig.1. We can thus divide the various types of RPV one-loop exchanges into two categories, type A and type B, according to the pair of RPV couplings involved:

Type A: The RPV contributions that are proportional to the product $\lambda'\lambda'$, i.e., $\Gamma(Z \rightarrow d_I \bar{d}_J) \propto \lambda'\lambda'$, where λ' is defined in (51).

Type B: The RPV contributions that are proportional to the product $b\lambda'$, i.e., $\Gamma(Z \rightarrow d_I \bar{d}_J) \propto b\lambda'$, where b is the soft breaking RPV bilinear coupling defined in (53).

A. Type A RPV effect

The type A RPV contribution to $Z \rightarrow d_I \bar{d}_J$ emanates from the first five RPV Yukawa-like interaction vertices in (54). In this case we assume that $b_i \rightarrow 0$ such that mixing effects between sleptons and the Higgs fields are absent.

We can further sub-divide the type A contributions into 6 types according to the type of scalar (S) and type of fermion (f) that are being exchanged in the loops:

$$\begin{aligned} \text{type A1 : } & S_\alpha = \tilde{e}_{L,\alpha} \quad , \quad f_i = u_i \\ \text{type A2 : } & S_\alpha = \tilde{d}_{L,\alpha} \quad , \quad f_i = \nu_i \end{aligned}$$

Thus, for example $m_{\tilde{u}_i}(\delta_M^U = 0.9, \delta_A^U = 0) = m_{\tilde{u}_i}(\delta_M^U = 0, \delta_A^U = 0.9)$, $i = 1, 2, 3$ and 4.

[6] Note that at the one-loop level the λ type couplings do not contribute to the decay $Z \rightarrow d_I \bar{d}_J$.

[7] The one-loop exchanges of possible lepton-chargino and neutrino-neutralino admixture states in $Z \rightarrow d_I \bar{d}_J$ will be controlled by the square of the RPV couplings product $\mu_i \times \lambda'$.

$$\begin{aligned}
\text{type A3: } & S_\alpha = \tilde{d}_{R,\alpha} \ , \ f_i = \nu_i^c \\
\text{type A4: } & S_\alpha = \tilde{\nu}_{L,\alpha} \ , \ f_i = d_i \\
\text{type A5: } & S_\alpha = \tilde{\nu}_{L,\alpha}^* \ , \ f_i = d_i \\
\text{type A6: } & S_\alpha = \tilde{u}_{L,\alpha} \ , \ f_i = e_i \ , \quad (55)
\end{aligned}$$

where $\alpha = 1, 2, 3$ and $i = 1, 2, 3$.

For each of the type A RPV exchanges above, the generic couplings defined in (2), (7) and (8) are summarized in Table IV. In particular, for a given f , the Zff couplings of (2) are given by (3)-(6). The Sdf couplings are taken from the Yukawa like interactions in (54), while the ZSS couplings are extracted from $\mathcal{L}(V_\mu \tilde{u} \tilde{u})$ in (46), from $\mathcal{L}(V_\mu \tilde{d} \tilde{d})$ in (42) and from the $V\tilde{L}\tilde{L}$ interaction Lagrangian:

$$\mathcal{L}(V_\mu \tilde{L} \tilde{L}) = -i \frac{1}{2} \tilde{L}_\ell^\star \left[\frac{e}{s_W} \tau^3 A_\mu^3 - \frac{e}{c_W} B_\mu \right] \overleftrightarrow{\partial}_L^\mu \tilde{L}_\ell \ , \quad (56)$$

where A^3 and B are the SU(2) and U(1) gauge fields, respectively, $\tilde{L} = \begin{pmatrix} \tilde{\nu}_L \\ \tilde{e}_L \end{pmatrix}$ and $\tau^3 = \begin{pmatrix} 1 & 0 \\ 0 & -1 \end{pmatrix}$.

Given the couplings in Table IV and the structure of the form factors in (10)-(15) it is evident that there are only two types of $\lambda' \lambda'$ product combinations which enter the type A RPV contribution to the decay $Z \rightarrow d_I \bar{d}_J$:

1. The product $\lambda'_{mIn} \lambda'^*_{mJn}$. Types A1, A2, A5 and A6 are proportional to this couplings product.

2. The product $\lambda'^*_{mIn} \lambda'_{mJn}$. Types A3 and A4 are proportional to this couplings product.

Furthermore, since none of the scalars have both a left and a right handed RPVT coupling to fermions in the type A scenario, i.e., in the notation of (8) either $b_{L(\alpha)}^{ij} = 0$ or $b_{R(\alpha)}^{ij} = 0$ (see Table IV), the form factors $B_{L,k}^{IJ}$ and $B_{R,k}^{IJ}$ in the amplitude (9) (which requires a non-zero value for both the left and the right handed scalar-fermion-down quark couplings) vanish. Also, since $b_{L(\alpha)}^{ij} = 0$ for the RPV contributions of types A1, A2, A5 and A6, they contribute only to the right-handed vector-like form factor $A_{R,k}^{IJ}$. Similarly, the RPV contributions of types A3 and A4 have $b_{R(\alpha)}^{ij} = 0$, therefore, contributing only to $A_{L,k}^{IJ}$.

It should be noted that for any one of the type A RPV exchanges, if the scalars of different flavors that are being exchanged in the loops are degenerate and upon neglecting all fermion masses except for the top-quark, then there remain only three distinct types of contributions of the λ' products in the type A RPV scenario. That is, under this assumption $BR(Z \rightarrow d_I \bar{d}_J)$ can have only three different values which we denote by $BR1^{IJ}$, $BR2^{IJ}$ and $BR3^{IJ}$ as follows:

$$BR1^{IJ} = BR(Z \rightarrow d_I \bar{d}_J) \text{ when } (\lambda'_{iI} \times \lambda'_{iJ})^2 \neq 0 ; j \neq 3, i = 1, 2, 3 \quad (57)$$

$$BR2^{IJ} = BR(Z \rightarrow d_I \bar{d}_J) \text{ when } (\lambda'_{i3I} \times \lambda'_{i3J})^2 \neq 0 ; i = 1, 2, 3 \quad (58)$$

$$BR3^{IJ} = BR(Z \rightarrow d_I \bar{d}_J) \text{ when } (\lambda'_{iIj} \times \lambda'_{iJj})^2 \neq 0 ; i, j = 1, 2, 3 , \quad (59)$$

such that $BR(Z \rightarrow b \bar{s}) = BR1^{32}$, $BR2^{32}$ or $BR3^{32}$ depending on which of the three $\lambda' \lambda'$ product combinations is non-zero.

In Table V we give a sample of our numerical results for the three BR's in (57)-(59) scaled by the square of the appropriate $\lambda' \lambda'$ product. The results presented in Table V correspond to the case of a single non-zero $\lambda' \lambda'$ product (one index combination) contributing to each of the BR's $BR1^{32}$, $BR2^{32}$ and $BR3^{32}$. In addition, the masses of the squark and slepton being exchange in the loop (for a given index combination of the corresponding $\lambda' \lambda'$ product) are set to either $m_{\tilde{q}} = 500$ GeV with $m_{\tilde{\ell}} = 200$ GeV or $m_{\tilde{q}} = 1000$ GeV with $m_{\tilde{\ell}} = 500$ GeV.

The existing limits on the λ' coupling products in (57)-(59) seem to indicate that the typical allowed values of $\lambda' \times \lambda'$ for any of the index combinations in (57)-(59) is at the level of $\sim \text{few} \times 10^{-2}$ [33]. It should be noted, however, that the limits reported in [33] assume 100

GeV scalar masses. These limits scale with the scalar masses (typically as $[m_{\tilde{s}}/100 \text{ GeV}]^2$, where $m_{\tilde{s}}$ is the scalar mass) and are, therefore, relaxed as the scalars become heavier.^[8]

Using $\lambda' \times \lambda' \sim \mathcal{O}(10^{-2})$ in conjunction with the results presented in Table V, we see that the expected branching ratio for $Z \rightarrow b \bar{s}$ in the type A RPV scenario investigated in this section lies in the range $BR(Z \rightarrow d_I \bar{d}_J) \sim 10^{-11} - 10^{-10}$.

This type A RPV one-loop effect in $BR(Z \rightarrow d_I \bar{d}_J)$ was also investigated in [6]. Although [6] evaluated some distinct limiting cases of the type A RPV contributions,

[8] Note that $b \rightarrow s \gamma$, which is proportional to $\lambda' \times \lambda'$ products with the same index combinations as in $Z \rightarrow b \bar{s}$, allows some of the above $\lambda' \times \lambda'$ coupling products to be at the 10^{-1} level [34].

	type A1	type A2	type A3
scalar (S_α)	$\tilde{e}_{L,\alpha}, \alpha = 1, 2$	$\tilde{d}_{L,\alpha}, \alpha = 1, 2, 3$	$\tilde{d}_{R,\alpha}, \alpha = 1, 2, 3$
fermion (f_i)	$u_i, i = 1, 2, 3$	$\nu_i, i = 1, 2, 3$	$\nu_i^c, i = 1, 2, 3$
$a_{L(Zf)}^{ij}$	$a_{L(Zu)}$	$a_{L(Z\nu)}$	$-a_{R(Z\nu)}$
$a_{R(Zf)}^{ij}$	$a_{R(Zu)}$	$a_{R(Z\nu)}$	$-a_{L(Z\nu)}$
$b_{L(\alpha)}^{ij}$	0	0	$\lambda'_{ij\alpha}$
$b_{R(\alpha)}^{ij}$	$-\lambda'^*_{\alpha ij}$	$\lambda'^*_{i\alpha j}$	0
$g_Z^{\alpha\beta}$	$-e \frac{c_W^2 - s_W^2}{2s_W c_W} \delta_{\alpha\beta}$	$-\frac{e}{2s_W c_W} (1 - \frac{2}{3}s_W^2) \delta_{\alpha\beta}$	$\frac{1}{3}e \frac{s_W}{c_W} \delta_{\alpha\beta}$

	type A4	type A5	type A6
scalar (S_α)	$\tilde{\nu}_{L,\alpha}, \alpha = 1, 2$	$\tilde{\nu}_{L,\alpha}^*, \alpha = 1, 2$	$\tilde{u}_{L,\alpha}, \alpha = 1, 2, 3$
fermion (f_i)	$d_i, i = 1, 2, 3$	$d_i, i = 1, 2, 3$	$e_i, i = 1, 2, 3$
$a_{L(Zf)}^{ij}$	$a_{L(Zd)}$	$a_{L(Zd)}$	$a_{L(Ze)}$
$a_{R(Zf)}^{ij}$	$a_{R(Zd)}$	$a_{R(Zd)}$	$a_{R(Ze)}$
$b_{L(\alpha)}^{ij}$	$\lambda'_{\alpha j i}$	0	0
$b_{R(\alpha)}^{ij}$	0	$\lambda'^*_{\alpha i j}$	$-\lambda'^*_{i\alpha j}$
$g_Z^{\alpha\beta}$	$-\frac{e}{2s_W c_W} \delta_{\alpha\beta}$	$\frac{e}{2s_W c_W} \delta_{\alpha\beta}$	$\frac{e}{2s_W c_W} (1 - \frac{4}{3}s_W^2) \delta_{\alpha\beta}$

TABLE IV: The couplings required for the calculation of $\Gamma(Z \rightarrow d_I \bar{d}_J)$ in the type A RPV scenario. The couplings follow the notation in (2)-(8).

	$\frac{BR1^{32}}{(\lambda'_{ij3} \times \lambda'_{ij2})^2}, j \neq 3$	$\frac{BR2^{32}}{(\lambda'_{i33} \times \lambda'_{i32})^2}$	$\frac{BR3^{32}}{(\lambda'_{i3j} \times \lambda'_{i2j})^2}$
$m_{\tilde{q}} = 500 \text{ GeV}, m_{\tilde{\ell}} = 200 \text{ GeV}$	4.2×10^{-7}	2.4×10^{-6}	3.4×10^{-6}
$m_{\tilde{q}} = 1000 \text{ GeV}, m_{\tilde{\ell}} = 500 \text{ GeV}$	3.9×10^{-7}	6.4×10^{-8}	3.0×10^{-6}

TABLE V: Results for the three types of branching ratios $BR1^{32}$, $BR2^{32}$, $BR3^{32}$ as defined in (57)-(59), each scaled by its appropriate $\lambda'\lambda'$ coupling product. Results are given for two sets of squark and slepton masses as indicated.

our results agree with the highlights of their analysis, i.e., that the typical $BR(Z \rightarrow d_I \bar{d}_J)$ is expected to be at the level of $10^{-11} - 10^{-10}$ if $\lambda' \times \lambda' \sim \mathcal{O}(10^{-2})$.

Thus, the type A RPV scenario is expected to yield a BR smaller even from the SM one. We, therefore, proceed below to the second RPV type B scenario which seems to give a much larger $BR(Z \rightarrow b \bar{s})$ within the ex-

perimentally allowed range of values for its relevant RPV parameter space.

B. Type B RPV effect

The type B RPV effect arises when a Higgs particle that is being exchanged in the loops mixes with a slepton through the RPVB operator in (53) and then couples to the external down quark via a λ' type coupling.

For simplicity we will assume that $b_i \neq 0$ only for $i = 3$ in (53), thus, considering only the mixing between the third generation sleptons (\tilde{L}_3) and the Higgs scalar fields (H_d and H_u).^[9] It should be noted that $b_3 \neq 0$ leads in general to a non-vanishing tau-sneutrino VEV, v_3 . However, since lepton number is not a conserved quantum number in this scenario, the \hat{H}_d and \hat{L}_3 superfields lose their identity and can be rotated to a particular basis (\hat{H}'_d, \hat{L}'_3) in which either μ_3 or v_3 are set to zero [26, 28, 32, 35]. In what follows, we find it convenient to choose the “no VEV” basis, $v_3 = 0$, which simplifies our analysis below.

Let us define the SU(2) components of the up-type

Higgs, down-type Higgs and \tilde{L}_3 scalar doublet fields (setting $v_3 = 0$):

$$\begin{aligned} H_u &\equiv \begin{pmatrix} h_u^+ \\ (\xi_u^0 + v_u + i\phi_u^0)/\sqrt{2} \end{pmatrix}, \\ H_d &\equiv \begin{pmatrix} (\xi_d^0 + v_d + i\phi_d^0)/\sqrt{2} \\ h_d^- \end{pmatrix}, \\ \tilde{L}_3 &\equiv \begin{pmatrix} (\tilde{\nu}_+^0 + i\tilde{\nu}_-^0)/\sqrt{2} \\ \tilde{e}_3^- \end{pmatrix}, \end{aligned} \quad (60)$$

where $\tilde{\nu}_+^0$, $\tilde{\nu}_-^0$ and \tilde{e}_3^- are the SU(2) CP-even, CP-odd τ -sneutrino and left handed stau fields, respectively.

When $b_3 \neq 0$ the 3rd generation slepton SU(2) fields in (60) mix with the Higgs fields. In particular, in the basis $\Phi_C^0 = (h_u^+, h_d^+, \tilde{e}_3^+)$, the squared mass matrix in the charged scalar sector becomes:^[10]

$$M_C^2 = \begin{pmatrix} c_\beta^2 [(m_A^0)^2 + m_W^2] & s_\beta c_\beta [(m_A^0)^2 + m_W^2] & b_3 \\ s_\beta c_\beta [(m_A^0)^2 + m_W^2] & s_\beta^2 [(m_A^0)^2 + m_W^2] & b_3 t_\beta \\ b_3 & b_3 t_\beta & (m_{s\nu}^0)^2 - m_W^2 \cos 2\beta \end{pmatrix}, \quad (61)$$

where m_A^0 and $m_{s\nu}^0$ are the pseudo-scalar Higgs mass and the tau-sneutrino mass, respectively, in the RPC limit $b_3 \rightarrow 0$.

Similarly, in the basis $\Phi_E^0 = (\xi_d^0, \xi_u^0, \tilde{\nu}_+^0)$, the CP-even neutral scalar squared mass matrix becomes (at tree-level):^[11]

$$M_E^2 = \begin{pmatrix} (m_A^0)^2 s_\beta^2 + m_Z^2 c_\beta^2 & -[(m_A^0)^2 + m_Z^2] s_\beta c_\beta & b_3 t_\beta \\ -[(m_A^0)^2 + m_Z^2] s_\beta c_\beta & (m_A^0)^2 c_\beta^2 + m_Z^2 s_\beta^2 & -b_3 \\ b_3 t_\beta & -b_3 & (m_{s\nu}^0)^2 \end{pmatrix}. \quad (62)$$

Finally, in the CP-odd neutral scalar sector and in the basis $\Phi_O^0 = (\phi_d^0, \phi_u^0, \tilde{\nu}_-^0)$ one obtains:

$$M_O^2 = \begin{pmatrix} (m_A^0)^2 c_\beta^2 & (m_A^0)^2 c_\beta s_\beta & b_3 t_\beta \\ (m_A^0)^2 c_\beta s_\beta & (m_A^0)^2 s_\beta^2 & b_3 \\ b_3 t_\beta & b_3 & (m_{s\nu}^0)^2 \end{pmatrix}. \quad (63)$$

The new charged scalar and CP-even and CP-odd neutral scalar mass-eigenstates (i.e., the physical states) are then derived by diagonalizing M_C^2 , M_E^2 and M_O^2 , respectively. Let us denote the physical states by:

$$\Phi_C = \begin{pmatrix} H^+ \\ G^+ \\ \tilde{\tau}^+ \end{pmatrix}, \quad \Phi_E = \begin{pmatrix} H \\ h \\ \tilde{\nu}_+^\tau \end{pmatrix}, \quad \Phi_O = \begin{pmatrix} A \\ G \\ \tilde{\nu}_-^\tau \end{pmatrix}, \quad (64)$$

tional mixings among sleptons of different generations and mixings between the selectron and/or smuon scalar doublets with the Higgs fields. These extra mixing effects are not crucial for the main outcome of this section.

[10] We neglect the mixing between the right-handed SU(2) stau singlet and the charged Higgs fields which is proportional to the tau mass.

[11] The one loop corrections to the 2×2 Higgs block in M_E^2 can cause a significant deviation to the tree-level mass of the light Higgs. This effect will be discussed below.

[9] The consequences of $b_1 \neq 0$ and/or $b_2 \neq 0$ is to introduce addi-

such that, for a small RPVB in the scalar potential, the new physical states in (64) are the states dominated by what would be the corresponding physical states in the RPC limit, $b_3 = 0$, for which the Higgs sector decouples from the slepton sector in (61), (62) and (63). In particular, if $b_3 \rightarrow 0$, then H , h , A and H^\pm become the usual RPC MSSM's CP-even heavy Higgs, CP-even light Higgs, CP-odd pseudo-scalar Higgs and charged Higgs states, respectively. Similarly, in this limit $\tilde{\nu}_+^\tau$ and $\tilde{\nu}_-^\tau$ become the two mass-degenerate CP-even and CP-odd sneutrino states with a common mass $m_{\tilde{\nu}_+^\tau} = m_{\tilde{\nu}_-^\tau} \equiv m_{s\nu}^0$, while $\tilde{\tau}^+$ is the usual pure left handed stau field with a mass $m_{\tilde{\tau}^+} = \sqrt{(m_{s\nu}^0)^2 - m_W^2 \cos 2\beta}$. Note also that G and G^\pm are the neutral and charged Goldstone bosons that are absorbed by the Z and W -bosons and are, therefore, the states with a zero eigenvalue in M_O^2 and M_C^2 , respectively.

The physical states Φ_C , Φ_E and Φ_O are related to the weak states Φ_C^0 , Φ_E^0 and Φ_O^0 via:

$$\begin{aligned}\Phi_{C,i}^0 &= R_{C,ik} \Phi_{C,k}, \\ \Phi_{E,i}^0 &= R_{E,ik} \Phi_{E,k}, \\ \Phi_{O,i}^0 &= R_{O,ik} \Phi_{O,k},\end{aligned}\quad (65)$$

where R_C , R_E and R_O are the rotation matrices that diagonalize M_C^2 , M_E^2 and M_O^2 , respectively.

Notice that the mass matrices M_C^2 , M_E^2 and M_O^2 depend only on four SUSY parameters: m_A^0 , $m_{s\nu}^0$, b_3 and $\tan\beta$. These parameters, therefore, completely fix the rotation matrices R_C , R_O and R_E from which the CP-even and CP-odd neutral scalar spectrum as well as the charged scalar spectrum is completely determined.

Clearly then, the type B RPV contributions involve the 3rd generation sleptons that can mix with the Higgs fields through a b_3 bilinear RPV coupling which enters the slepton-Higgs mixed mass matrices in (61)-(63). Here also, we can further sub-divide the type B RPV effects according to the type of scalar (S) and type of fermion (f) that are being exchanged in the loops:

$$\text{type B1: } S_\alpha = \Phi_{C,\alpha}; \quad f_i = u_i, \quad (66)$$

with $\alpha = 1, 3$, $i = 1, 2, 3$ and

$$\text{type B2: } S_\alpha = \Phi_{E,\alpha} \text{ and } \Phi_{O,\beta}; \quad f_i = d_i, \quad (67)$$

with $\alpha = 1, 2, 3$, $\beta = 1, 3$, $i = 1, 2, 3$.

Note that we have omitted virtual exchanges of the two Goldstone bosons G and G^\pm since the one-loop amplitudes are being calculated in the unitary gauge.

The two RPV effects, of types B1 and B2 above, are driven by the Higgs-slepton scalar admixtures Φ_C , Φ_E , Φ_O which couple to quarks through a combination of λ' and Higgs Yukawa coupling. Hence, the Higgs-like components in Φ_C , Φ_E and Φ_O will couple through the Higgs Yukawa terms, while the slepton-like component interact with the quarks via the λ' -type RPV couplings in (54).

For the type B1 RPV contribution in (66) the form factors defined in (9) are calculated following the prescription described in section II. The generic couplings defined in (2), (7) and (8) are summarized in Table VI for the type B1 RPV exchanges. In particular, the Sdf couplings (for $S = \Phi_C$ and $f = u$) are a combination of the Yukawa-like trilinear RPV interactions in (54) (those with the third generation slepton indices) and the charged Higgs Yukawa couplings which are the same as in the 2HDM of type II (given in section III).

The ZSS couplings (for $S = \Phi_C$) in Table VI are derived from $\mathcal{L}(V_\mu \tilde{L}_3 \tilde{L}_3)$ in (56) and from the following $\mathcal{L}(V_\mu H_d H_d)$ and $\mathcal{L}(V_\mu H_u H_u)$ pieces [22]:

$$\mathcal{L}(V_\mu H_d H_d) = -i \frac{1}{2} H_d^\star \left[\frac{e}{s_W} \tau^3 A_\mu^3 - \frac{e}{c_W} B_\mu \right] \partial_H^{\mu \leftrightarrow} H_d, \quad (68)$$

$$\mathcal{L}(V_\mu H_u H_u) = -i \frac{1}{2} H_u^\star \left[\frac{e}{s_W} \tau^3 A_\mu^3 + \frac{e}{c_W} B_\mu \right] \partial_H^{\mu \leftrightarrow} H_u, \quad (69)$$

where the SU(2) scalar doublet fields \tilde{L}_3 , H_d and H_u are defined in (60).

	type B1
scalar (S_α)	$\Phi_{C,\alpha}, \quad \alpha = 1, 3$
fermion (f_i)	$u_i, \quad i = 1, 2, 3$
$a_{L(Zf)}^{ij}$	$a_{L(Zu)}$
$a_{R(Zf)}^{ij}$	$a_{R(Zu)}$
$b_{L(\alpha)}^{ij}$	$\frac{e}{\sqrt{2}s_W} \frac{m_{u_i}}{m_W c_\beta} R_C^{1\alpha} V_{ij}$
$b_{R(\alpha)}^{ij}$	$\frac{e}{\sqrt{2}s_W} \frac{m_{d_j}}{m_W c_\beta} R_C^{2\alpha} V_{ij} - \lambda_{3ij}' R_C^{3\alpha}$
$g_Z^{\alpha\beta}$	$-e \cot 2\theta_W \delta_{\alpha\beta}$

TABLE VI: The couplings required for the calculation of $\Gamma(Z \rightarrow d_I \bar{d}_J)$ in the type B1 RPV scenario. The couplings follow the notation in (2), (7) and (8). The couplings $a_{L,R(Zu)}$ are given in (3)-(6).

For the type B2 RPV case (see (67)) there are 10 one-loop diagrams that can potentially contribute to the decay $Z \rightarrow d_I \bar{d}_J$. These diagrams are depicted in Fig. 10. The first eight diagrams in Fig. 10 have the same topology as the generic diagrams of Fig. 1, while diagrams 9 and 10 involve virtual exchanges of a Z -boson through the $ZZ\Phi_E$ interaction.

Using our generic notation for the one-loop amplitude in (9), we calculate the form factors $A_{L,k}^{IJ}$, $A_{R,k}^{IJ}$ and $B_{L,k}^{IJ}$, $B_{R,k}^{IJ}$ with $k = 1-10$, which emerge from diagrams 1-10 in Fig. 10 (taking $m_{d_i} = 0$, for d , s and b -quarks):

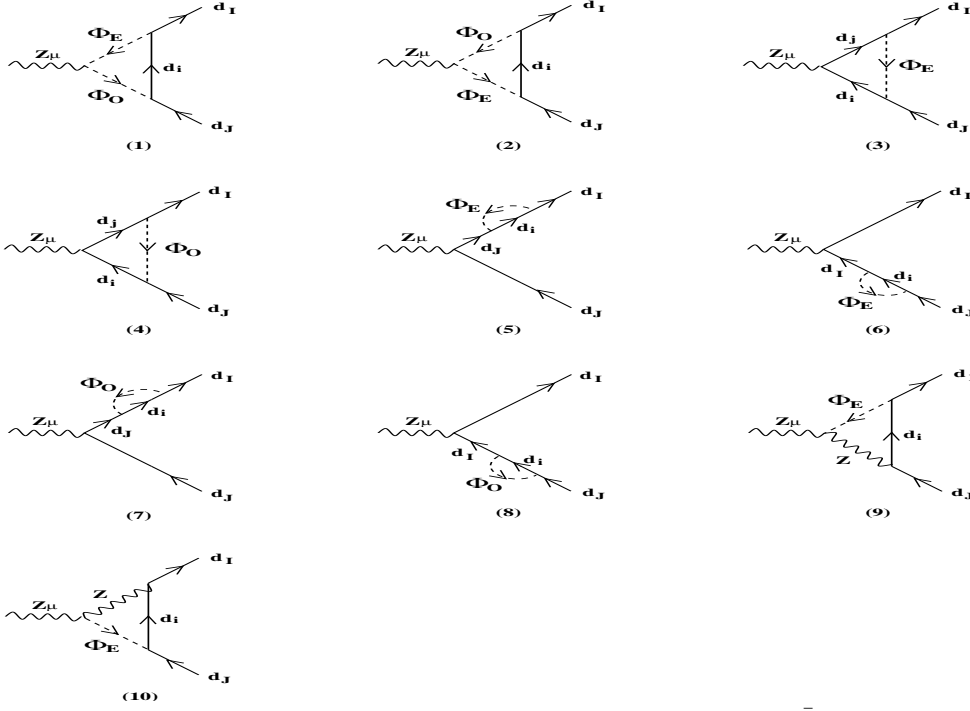


FIG. 10: One-loop diagrams that contribute to the flavor changing decays $Z \rightarrow d_I \bar{d}_J$ in the type B2 RPV scenario.

$$A_{L,1}^{IJ} = -2 \sum_{\alpha,\beta,i} g_Z^{\alpha\beta} b_{L(\alpha)}^{(E)iI} b_{L(\beta)}^{(O)iJ} C_{24}^1, \quad (70)$$

$$A_{L,2}^{IJ} = 2 \sum_{\alpha,\beta,i} g_Z^{\beta\alpha} b_{L(\alpha)}^{(O)iI} b_{L(\beta)}^{(E)iJ} C_{24}^2, \quad (71)$$

$$A_{L,3}^{IJ} = a_{R(Zd)} \sum_{\alpha,i,j} b_{L(\alpha)}^{(E)iI} b_{L(\alpha)}^{(E)jJ} [2C_{24}^3 - m_Z^2 (C_{23}^3 - C_{22}^3)], \quad (72)$$

$$A_{L,4}^{IJ} = a_{R(Zd)} \sum_{\alpha,i,j} b_{L(\alpha)}^{(O)iI} b_{L(\alpha)}^{(O)jJ} [2C_{24}^4 - m_Z^2 (C_{23}^4 - C_{22}^4)], \quad (73)$$

$$A_{L,56}^{IJ} = a_{L(Zd)} \sum_{\alpha,i} b_{L(\alpha)}^{(E)iI} b_{L(\alpha)}^{(E)iJ} B_1^5, \quad (74)$$

$$A_{L,78}^{IJ} = a_{L(Zd)} \sum_{\alpha,i} b_{L(\alpha)}^{(O)iI} b_{L(\alpha)}^{(O)iJ} B_1^7, \quad (75)$$

$$A_{L,9}^{IJ} = A_{L,10}^{IJ} = 0, \quad (76)$$

where we have combined the contribution of the self energy diagrams 5+6 and 7+8: $\mathcal{M}_5 + \mathcal{M}_6 \equiv \mathcal{M}_{56}$ and $\mathcal{M}_7 + \mathcal{M}_8 \equiv \mathcal{M}_{78}$, which leads accordingly to $A_{L,5}^{IJ} + A_{L,6}^{IJ} \equiv A_{L,56}^{IJ}$ and $A_{L,7}^{IJ} + A_{L,8}^{IJ} \equiv A_{L,78}^{IJ}$. Also,

$$B_{L,k}^{IJ} = 0 \text{ for } k = 1 - 8 \quad (77)$$

$$B_{L,9}^{IJ} = a_{L(Zd)} \sum_{\alpha} g_{ZZ\Phi_E}^{\alpha} b_{L(\alpha)}^{(E)IJ} [2(C_{12}^9 - C_{11}^9) + \frac{1}{m_Z^2} (\tilde{C}_0^9 + \tilde{C}_{11}^9)], \quad (78)$$

$$B_{L,10}^{IJ} = a_{R(Zd)} \sum_{\alpha} g_{ZZ\Phi_E}^{\alpha} b_{L(\alpha)}^{(E)IJ} [2(C_{12}^{10} - C_{11}^{10}) + \frac{1}{m_Z^2} (\tilde{C}_0^{10} + \tilde{C}_{11}^{10})]. \quad (79)$$

Here also the right-handed form factors, $A_{R,k}^{IJ}$ and $B_{R,k}^{IJ}$, are obtained from the corresponding left handed ones by interchanging $L \rightarrow R$ and $R \rightarrow L$ in all the couplings in (70)-(79).

The two-point and three-point loop form factors B_1^k with $k = 5, 7$, C_x^k with $x \in 11, 12, 21, 22, 23, 24$ and $k = 1, 2, 3, 4, 9, 10$ and \tilde{C}_x^k with $x \in 0, 11, 12$ and $k = 9, 10$ which appear in (70)-(79) are given by:

$$B_1^5 = B_1(m_{d_i}^2, m_{\Phi_{E,\alpha}}^2, m_{d_I}^2), \quad (80)$$

$$B_1^7 = B_1(m_{d_i}^2, m_{\Phi_{O,\alpha}}^2, m_{d_I}^2), \quad (81)$$

and

$$C_x^1 = C_x(m_{d_i}^2, m_{\Phi_{E,\alpha}}^2, m_{\Phi_{O,\beta}}^2, m_{d_I}^2, q^2, m_{d_J}^2), \quad (82)$$

$$C_x^2 = C_x(m_{d_i}^2, m_{\Phi_{O,\alpha}}^2, m_{\Phi_{E,\beta}}^2, m_{d_I}^2, q^2, m_{d_J}^2), \quad (83)$$

$$C_x^3 = C_x(m_{\Phi_{E,\alpha}}^2, m_{d_i}^2, m_{d_J}^2, m_{d_J}^2, q^2, m_{d_I}^2), \quad (84)$$

$$C_x^4 = C_x(m_{\Phi_{O,\alpha}}^2, m_{d_i}^2, m_{d_J}^2, m_{d_J}^2, q^2, m_{d_I}^2), \quad (85)$$

$$C_x^9; \tilde{C}_x^9 = C_x; \tilde{C}_x \left(m_{d_J}^2, m_Z^2, m_{\Phi_{E,\alpha}}^2, m_{d_J}^2, q^2, m_{d_I}^2 \right), \quad (86)$$

$$C_x^{10}; \tilde{C}_x^{10} = C_x; \tilde{C}_x \left(m_{d_I}^2, m_Z^2, m_{\Phi_{E,\alpha}}^2, m_{d_I}^2, q^2, m_{d_J}^2 \right), \quad (87)$$

where $B_1(m_1^2, m_2^2, p^2)$, $C_x(m_1^2, m_2^2, m_3^2, p_1^2, p_2^2, p_3^2)$ and $\tilde{C}_x(m_1^2, m_2^2, m_3^2, p_1^2, p_2^2, p_3^2)$ are defined in the appendix.

The couplings $a_{L(Zd)}$, $a_{R(Zd)}$, $b_{L(\alpha)}^{(E)ij}$, $b_{R(\alpha)}^{(E)ij}$, $b_{L(\alpha)}^{(O)ij}$, $b_{R(\alpha)}^{(O)ij}$, $g_Z^{\alpha\beta}$ and $g_{ZZ\Phi_E}^\alpha$ needed for evaluating the form factors above are given in Table VII. In particular, $a_{L,R(Zd)}$ are the SM left and right-handed couplings of the Z-boson to a pair of down quarks as given in (3)-(6). The rest are obtained from the relevant interaction Lagrangian terms by rotating the SU(2) weak states $\Phi_{C,E,O}^0$ to the physical states $\Phi_{C,E,O}$ according to (65). In particular, the $\Phi_E \bar{d}_i d_j$ couplings $b_{L,R(\alpha)}^{(E)ij}$ and $\Phi_O \bar{d}_i d_j$ couplings $b_{L,R(\alpha)}^{(O)ij}$ follow the notation of the generic Sdf vertex in (8); for $S = \Phi_E$ or Φ_O and $f = d$:

$$\Lambda(\Phi_{E,\alpha} \bar{d}_i d_j) = i \left(b_{L(\alpha)}^{(E)ij} L + b_{R(\alpha)}^{(E)ij} R \right), \quad (88)$$

$$\Lambda(\Phi_{O,\alpha} \bar{d}_i d_j) = i \left(b_{L(\alpha)}^{(O)ij} L + b_{R(\alpha)}^{(O)ij} R \right). \quad (89)$$

These couplings emanate from both the Yukawa-like trilinear RPV interactions in (54) and the neutral Higgs Yukawa vertices of a 2HDM of type II as given in (23).

The coupling $g_Z^{\alpha\beta}$ of a Z-boson to a $\Phi_{E,\alpha} \Phi_{O,\beta}$ pair follow our generic definition of the VSS vertex in (7). It is derived from the Lagrangian terms in (56), (68) and (69).

The coupling $g_{ZZ\Phi_E}^\alpha$ of $\Phi_{E,\alpha}$ to a pair of Z-bosons is defined as:

$$\Lambda(Z_\mu Z_\nu \Phi_{E,\alpha}) = i g_{ZZ\Phi_E}^\alpha g_{\mu\nu}, \quad (90)$$

and is obtained from the following $ZZ\xi_d^0$ and $ZZ\xi_u^0$ interaction terms (recall that $\xi_{d,u}^0$ are the CP-even SU(2) components of $H_{d,u}$ as defined in (60)) [22]:

$$\mathcal{L}(ZZ\xi_{d,u}^0) = \frac{e^2}{(2s_W c_W)^2} Z_\mu Z^\mu (v_d \xi_d^0 + v_u \xi_u^0), \quad (91)$$

where v_d and v_u are the VEV's of the down-type and up-type Higgs doublets, respectively.

Before presenting our numerical results for the type B RPV contribution let us discuss some of its salient features and outline the main assumptions and notations regarding the relevant parameter space involved:

- I. The pseudo-scalar “bare” mass (i.e., its mass in the RPC limit of $b_3 \rightarrow 0$) can be approximated from the tree-level relation which, for $t_\beta^2 \gg 1$, gives $(m_A^0)^2 \sim b_0 t_\beta$, where b_0 is the usual RPC soft-breaking bilinear Higgs term in the scalar potential, i.e., $V_{RPC} \supset b_0 H_d H_u$.

	type B2
scalar (S_α)	$\Phi_{E,\alpha}, \alpha = 1, 2, 3$ and $\Phi_{O,\alpha}, \alpha = 1, 3$
fermion (f_i)	$d_i, i = 1, 2, 3$
$a_{L(Zf)}^{ij}$	$a_{L(Zd)}$
$a_{R(Zf)}^{ij}$	$a_{R(Zd)}$
$b_{L(\alpha)}^{(E)ij}$	$-\frac{e}{2s_W} \frac{m_{d_i}}{m_W c_\beta} R_E^{1\alpha} \delta_{ij} + \frac{1}{\sqrt{2}} \lambda'_{3ji} R_E^{3\alpha}$
$b_{R(\alpha)}^{(E)ij}$	$-\frac{e}{2s_W} \frac{m_{d_i}}{m_W c_\beta} R_E^{1\alpha} \delta_{ij} + \frac{1}{\sqrt{2}} \lambda'^*_{3ij} R_E^{3\alpha}$
$b_{L(\alpha)}^{(O)ij}$	$-i \frac{e}{2s_W} \frac{m_{d_i}}{m_W c_\beta} R_O^{1\alpha} \delta_{ij} + \frac{i}{\sqrt{2}} \lambda'_{3ji} R_O^{3\alpha}$
$b_{R(\alpha)}^{(O)ij}$	$i \frac{e}{2s_W} \frac{m_{d_i}}{m_W c_\beta} R_O^{1\alpha} \delta_{ij} + \frac{i}{\sqrt{2}} \lambda'^*_{3ij} R_O^{3\alpha}$
$g_Z^{\alpha\beta}$	$i \frac{e}{\sin 2\theta_W} \left(R_E^{1\alpha} R_O^{1\beta} - R_E^{2\alpha} R_O^{2\beta} + R_E^{3\alpha} R_O^{3\beta} \right)$
$g_{ZZ\Phi_E}^\alpha$	$\frac{e}{s_W c_W} m_Z (c_\beta R_E^{1\alpha} + s_\beta R_E^{2\alpha})$

TABLE VII: The couplings required for the calculation of $\Gamma(Z \rightarrow d_I \bar{d}_J)$ in the type B2 RPV scenario. The couplings follow from the Feynman rules in (2), (7), (88), (89) and (90). The couplings $a_{L,R(Zd)}$ are given in (3)-(6).

Thus, without loss of generality, we trade the bilinear coupling b_3 with a dimensionless RPV parameter, ε , as follows:

$$b_3 \equiv \varepsilon (m_A^0)^2 \cot \beta, \quad (92)$$

such that $\varepsilon \sim \frac{b_3}{b_0}$ parametrizes the relative amount of RPV in the scalar potential. In particular, $\varepsilon \ll 1$ for small bilinear RPV and $\varepsilon \sim 1$ if RPV/RPC ~ 1 in the SUSY scalar sector.

The existing experimental limits on ε come from:

1. A non-vanishing b_3 can generate a radiative (one-loop) tau-neutrino mass. The laboratory limit on the tau-neutrino mass allows, however, the quantity $\frac{b_3}{b_0} \sim \varepsilon$ to be of $\sim \mathcal{O}(1)$ [28].
2. The parameter b_3 , or equivalently the quantity $\varepsilon \sim \frac{b_3}{b_0}$, can have important consequences on the CP-even and CP-odd Higgs-like scalar mass spectrum, see [36, 37]. In particular, ε can drive the mass of the physical CP-even light Higgs below its present LEP2 lower bound which, for $m_A \gtrsim 200$ GeV, is roughly

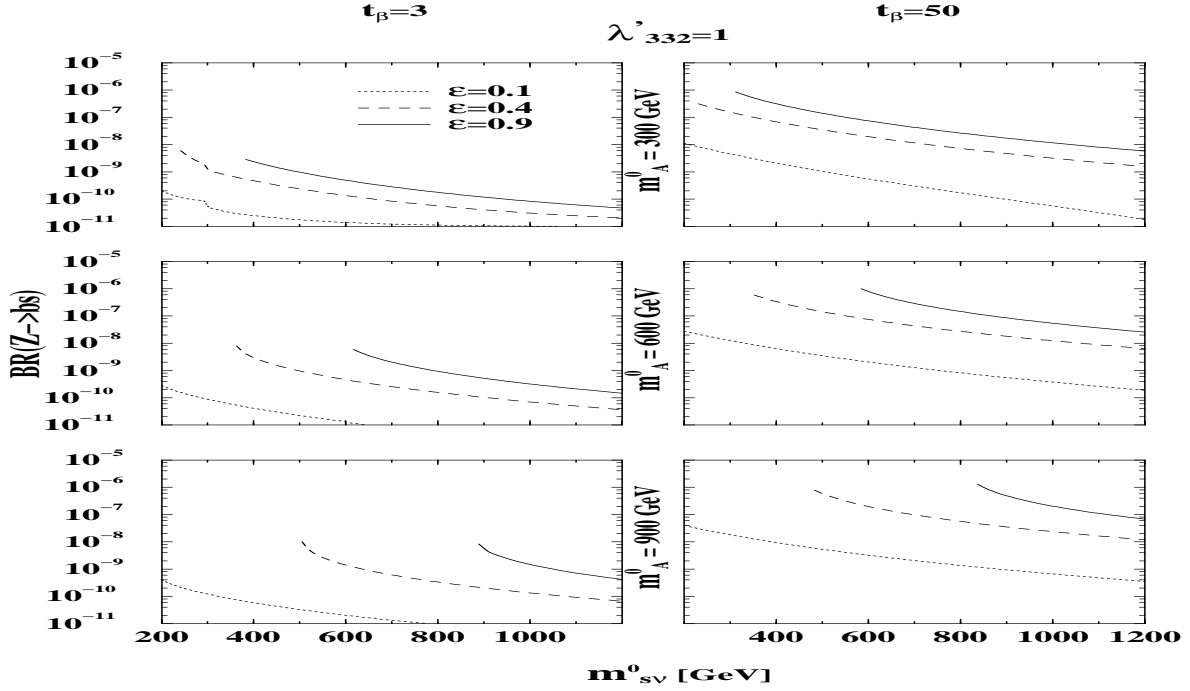


FIG. 11: $BR(Z \rightarrow b\bar{s} + \bar{s}b)$ as a function of the “bare” sneutrino mass parameter $m_{s\nu}^0$ (see text), for some combinations of values of m_A^0 and ε (as indicated in the figure) and for $t_\beta = 3$ (left plots) and $t_\beta = 50$ (right plots). $\lambda'_{332} = 1$ is used and ϵ is defined in (92).

$m_h \gtrsim 110$ GeV irrespective of $\tan\beta$ [38].^[12] Also, a non-zero ε can give rise to negative eigenvalues (i.e., to the physical square masses) for the CP-even and CP-odd mass matrices M_E^2 and M_O^2 in (62) and (63), depending on the values of the rest of the type B parameter space, i.e., on m_A^0 , $m_{s\nu}^0$ and t_β .

Therefore, in what follows, we will vary the parameters $\{m_A^0, m_{s\nu}^0, t_\beta, \varepsilon\}$ subject to the existing LEP2 lower bound on the light Higgs mass and to the requirement that $m_{\tilde{\nu}_\tau^\pm}$, $m_{\tilde{\nu}_\tau^\mp}$ and $m_{\tilde{\tau}^\pm}$ are > 150 GeV.

Since the light Higgs mass is very sensitive to higher order corrections to the 2×2 Higgs block in M_E^2 , as in [36, 37], in order to derive realistic exclusion regions for the parameter space $\{m_A^0, m_{s\nu}^0, t_\beta, \varepsilon\}$ through the requirement $m_h \gtrsim 110$ GeV, we include the dominant higher order corrections (coming from the $t-\bar{t}$ sector) to the (ξ_d^0, ξ_u^0) block in M_E^2 , following the approximate formulae given in [39] and taking the maximal mixing scenario with a typical squark mass of $m_{\tilde{q}} = 1$ TeV.

3. A non-vanishing ε can also alter the cross-section for ZZ and WW pair production through s -channel exchanges of the CP-even scalars Φ_E [36, 37]. The measured ZZ and WW cross-sections in LEP2 can thus be used to place limits on ε as a function of $\{m_A^0, m_{s\nu}^0, t_\beta\}$. These limits, however, can be evaded if the $\tilde{\nu}_\tau^\pm e^- e^+$ trilinear RPV coupling λ_{131} is assumed small enough (see [36, 37]). We will, therefore, not consider such limits below.

II. Since b_3 is not a flavor changing parameter, the transition between down-quarks of different generations, i.e., between the external down-quarks $d_I \rightarrow d_J$, is necessarily driven by a λ' coupling with the appropriate non-diagonal indices (disregarding flavor changing transitions due to small non-diagonal CKM elements). Thus, the type B RPV one-loop effect in $Z \rightarrow d_I \bar{d}_J$ is necessarily proportional to either $b_3 \lambda'_{3IJ}$ or $b_3 \lambda'_{3JI}$.

In particular, for $Z \rightarrow b\bar{s}$ we find that the dominant contribution is attributed to the type B1 exchanges of the charged scalars and it arises when $\lambda'_{332} \neq 0$. The only other possible index combination for $Z \rightarrow b\bar{s}$, which is $\lambda'_{323} \neq 0$, yields a much smaller branching ratio. This enhancement for the (332) index combination can be traced to the fact that, for this particular combination, the charged scalar amplitude involves also a top-quark exchange, thus gaining a factor of m_t/m_c compared to the $\lambda'_{323} \neq 0$ case (which involves a charm-quark exchange in the

[12] This bound is applicable in the maximal stop mixing scenario with a typical SUSY squark masses of 1 TeV. Note also that since $b_3 \neq 0$ the hZZ coupling is smaller than its value in the RPC case leading to a smaller $e^+e^- \rightarrow Zh$ production rate. Thus, the limits reported in [38] should be slightly relaxed in the type B RPV scenario.

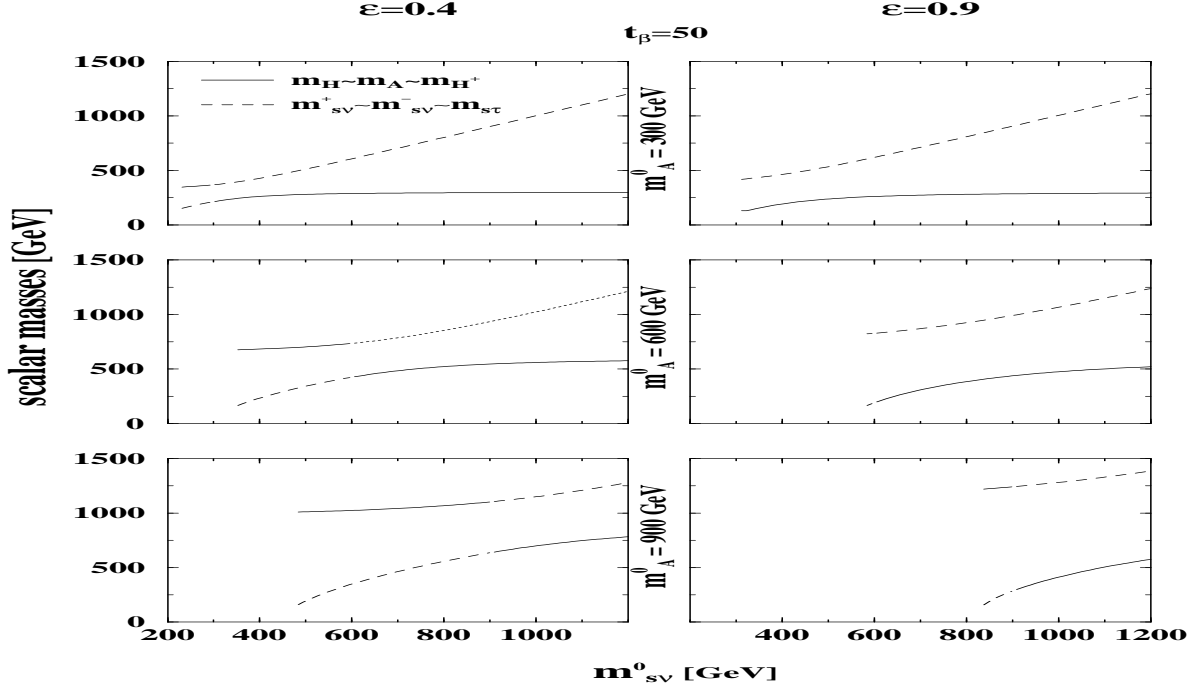


FIG. 12: Physical masses of the heavy CP-even Higgs (m_H), CP-odd Higgs (m_A), charged Higgs (m_{H^+}), CP-even tau-sneutrino ($m_{s\nu}^+$), CP-odd tau-sneutrino ($m_{s\nu}^-$) and the tau ($m_{s\tau}$), as a function of the “bare” tau-sneutrino mass ($m_{s\nu}^0$), for $t_\beta = 50$, for $m_A^0 = 300, 600$ or 900 GeV and for $\epsilon = 0.4$ (left figures) and $\epsilon = 0.9$ (right figures). ϵ is defined in (92).

loops).

III. In the limit $\epsilon \rightarrow 0$ the type B2 effect vanishes. However, since $\epsilon \rightarrow 0$ causes the charged Higgs sector to decouple from the stau sector and since the RPC MSSM Higgs sector is similar to the 2HDM of type II, the type B1 contribution approaches that of the type II 2HDM in this limit. Thus, for $\epsilon \rightarrow 0$, the type B1 RPV effect will be proportional to the off-diagonal CKM elements as in the case of the type II 2HDM discussed in section III.

IV. In the numerical analysis below we will set $\lambda'_{332} = 1$, while all other lambda’s with different index combinations are set to zero. The experimental limit on this coupling, derived from $R_\ell = \Gamma(Z \rightarrow \text{hadrons})/\Gamma(Z \rightarrow \ell\ell)$ [40], is (at the 2σ level) $\lambda'_{332} = 0.45$ for squark masses of ~ 100 GeV, while $\lambda'_{332} = 1$ is allowed for squark masses $\gtrsim 650$ GeV. The perturbativity bound on this coupling is $\lambda'_{332} = 1.04$ [41]. Thus, we will assume that the squarks are heavy enough to allow λ'_{332} to lie near its perturbativity limit (recall that no squarks are involved in the type B RPV contribution to $Z \rightarrow b\bar{s}$).

In Fig. 11 we show $BR(Z \rightarrow b\bar{s} + \bar{b}s)$ as a function of the “bare” tau-sneutrino mass $m_{s\nu}^0$ (i.e., what would be its mass in the RPC limit), for various possible values of m_A^0 , ϵ and for $t_\beta = 3$ (left side) and $t_\beta = 50$ (right side)

[24]. Evidently, $BR(Z \rightarrow b\bar{s} + \bar{b}s)$ is much larger in the high $\tan\beta$ scenario and it drops with $m_{s\nu}^0$.

The masses of the heavy CP-even Higgs, CP-odd Higgs and charged Higgs as well as the CP-even, CP-odd tau-sneutrino and the stau particles are depicted in Fig. 12, for $t_\beta = 50$ and for the same combinations of ϵ and m_A^0 that are used in Fig. 11. We note that in the limit $(m_A^0)^2 \gg m_Z^2$ (applicable to the values of m_A^0 in Figs. 11 and 12) one has $m_H \sim m_A \sim m_{H^+}$ and if in addition $(m_{s\nu}^0)^2 \gg m_Z^2$, then also the CP-even, CP-odd tau-sneutrinos and the stau are roughly degenerate. Thus, only two curves are shown in each plot in Figs. 12, which are sufficient to approximately describe all these six scalar masses.

Fig. 12 shows that at some instances, the Higgs-like and slepton-like scalar masses exhibit a discontinuous jump, at which point they “switch” identities. This phenomena is caused by the particular dependence of the physical scalar masses on the “bare” masses m_A^0 and $m_{s\nu}^0$ in the presence of $\epsilon \neq 0$. In particular, the corrections to the “bare” scalar masses due to a non-vanishing b_3 term are proportional to factors of $[(m_A^0) - (m_{s\nu}^0)]^{-1}$ (for more details see [36, 37]), thereby changing sign at the turning points. Moreover, the off-diagonal elements of the rotation matrices R_E , R_O and R_C , which are responsible for the slepton-Higgs mixings, are also inversely proportional to factors of $[(m_A^0) - (m_{s\nu}^0)]$, therefore, enhancing the type B RPV effect as m_A^0 approaches $m_{s\nu}^0$ as can be seen in Figs. 11.

model	scalars in the loops	$BR(Z \rightarrow b\bar{s})$
SM	W -boson (no scalars)	10^{-8}
2HDMII	charged Higgs	10^{-10}
T2HDM	charged Higgs	10^{-8}
SUSY with $\tilde{t} - \tilde{c}$ mixing	$\tilde{t} - \tilde{c}$ admixtures	10^{-8}
SUSY with $\tilde{b} - \tilde{s}$ mixing	$\tilde{b} - \tilde{s}$ admixtures	10^{-6}
SUSY with trilinear R_P -violation	squarks and sleptons	10^{-10}
SUSY with bilinear R_P -violation	slepton-Higgs admixtures	10^{-6}

TABLE VIII: The best case values for the branching ratio of $Z \rightarrow b\bar{s}$ for each of the six models considered in this paper upon imposing the available experimental limits on the relevant parameter space of each of them. The SM prediction is also given.

To summarize this section, with a large $\tan\beta$, a $BR(Z \rightarrow b\bar{s} + \bar{b}s) \sim \mathcal{O}(10^{-6})$ is possible within the type B scenario, e.g., for 40% lepton number violation in the SUSY scalar potential ($\varepsilon = 0.4$) and if the sleptons masses lie around ~ 200 GeV. For a heavier slepton spectrum a larger ε is required in order to push the branching ratio to the 10^{-6} level.

It should also be emphasized that since $BR(Z \rightarrow b\bar{s} + \bar{b}s)$ is dominated by the λ'_{332} , the decay $Z \rightarrow b\bar{s}$ is an efficient probe of this specific flavor changing trilinear RPV coupling.

VI. EXPERIMENTAL FEASIBILITY

In this section we will very briefly comment about the feasibility of observing (or achieving a limit) a signal of $Z \rightarrow b\bar{s}$ with a branching ratio of order 10^{-6} , at a Linear Collider producing 10^9 Z-bosons.

Such a signal should appear in the detector as an event with one b-jet and one light-jet (assuming no distinction is made between light = d, u or s -quarks). In the spirit of the analysis made with the 1993 and 1994 LEP data on $Z \rightarrow b\bar{s}$ [8], one defines ϵ_q^B and ϵ_q^L to be the efficiencies that a quark (or anti-quark) of flavor q is tagged as a b -jet (B) and light-jet (L), respectively. Thus, the key efficiency parameters for the detection of $Z \rightarrow b\bar{s}$ are ϵ_b^B , $\epsilon_{\text{light}}^L$ and ϵ_b^L , where the latter represent the probability that a b -jet is identified as a light-jet and is important for controlling the dominant background (to the $Z \rightarrow B + L$ signal) coming from $Z \rightarrow b\bar{b}$. Note, that due to the expected smallness of the "Purity" parameters $\epsilon_{\text{light}}^B$, ϵ_c^B and ϵ_c^L (see [8]), the background to $Z \rightarrow B + L$ caused by the SM $Z \rightarrow d\bar{d}$, $s\bar{s}$, $u\bar{u}$, $c\bar{c}$ decays will be sub-dominant.

With 10^9 Z-bosons, the expected number of events coming from $Z \rightarrow b\bar{s}$ (i.e., from new physics) and identi-

fied as $Z \rightarrow B + L$, is:

$$S \sim 10^9 \times \epsilon_b^B \epsilon_{\text{light}}^L BR(Z \rightarrow b\bar{s}) . \quad (93)$$

Similarly, the expected number of background $Z \rightarrow B + L$ events coming from the SM decay $Z \rightarrow b\bar{b}$ is:

$$B \sim 10^9 \times \epsilon_b^B \epsilon_b^L BR(Z \rightarrow b\bar{b}) . \quad (94)$$

Using (93) and (94), the expected statistical significance, S/\sqrt{B} , of the new physics signal $Z \rightarrow b\bar{s}$, with a branching ratio of order 10^{-6} , can reach beyond the 3-sigma level for $\epsilon_b^B \sim 0.6 - 0.8$, $\epsilon_{\text{light}}^L \sim 0.3 - 0.5$ and $\epsilon_b^L \sim \mathcal{O}(10^{-4})$. These values require an improvement to the 1993 and 1994 analysis [8], by a factor of 2-3 for ϵ_b^B and $\epsilon_{\text{light}}^L$ and by an order of magnitude for ϵ_b^L . With the expected advancement in the jet-tagging methods, in particular, for two-body decays of the Z-boson, these required values for the efficiency parameters above should be well within the reach of the future Linear Collider.

We can also get a clue about how low one can go in the value (or limit) of $BR(Z \rightarrow b\bar{s})$ with 10^9 Z-bosons, from the fact that the LEP preliminary results [8] achieved $BR(Z \rightarrow b\bar{s}) < \mathcal{O}(10^{-3})$ with $\mathcal{O}(10^6)$ Z-bosons. Scaling this limit, especially with the expected advance in b-tagging and identification of non-b jets methods, an $\mathcal{O}(10^{-6})$ branching ratios should be easily attained at a Giga-Z factory.

VII. SUMMARY

We have re-examined the flavor changing radiative decays of a Z-boson to a pair of down-quarks, $Z \rightarrow d_I \bar{d}_J$, with $I \neq J$. These Z-decay channels may prove useful in searching for new flavor physics beyond the SM at the

TESLA collider, or any other future collider, which may be designed to run on the Z-pole with high luminosities, thus accumulating more than 10^9 on-shell Z-bosons. With advances in technology, e.g., improved b-tagging efficiencies, the flavor changing decay $Z \rightarrow b\bar{s}$ - most likely the easiest to detect among the flavor changing hadronic Z-decays - may be accessible to a Giga-Z option even for branching ratios as small as $BR(Z \rightarrow b\bar{s}) \sim 10^{-7} - 10^{-6}$.

The $d_I \rightarrow d_J$ transition was assumed to be generated at one-loop through flavor violation in interactions between scalars and fermions.

A complete analytical derivation of the width $\Gamma(Z \rightarrow d_I \bar{d}_J)$ is presented using the form factor approach for the $Z d_I \bar{d}_J$ interaction vertex. These form factors are evaluated for the complete set of scalar-fermion one-loop exchanges with generic scalar-fermion flavor-violating couplings.

This prescription is then applied to the decay $Z \rightarrow b\bar{s}$ in six beyond the SM model scenarios for flavor-violation in the scalar sector:

1. Two Higgs doublet models with non-standard charged-Higgs couplings to quarks:
 - A two Higgs doublet model of type II (2HD-MII).
 - A two Higgs doublet model "for the top-quark" (T2HDM).
2. Supersymmetry with flavor-violation in the squark sector:
 - Supersymmetry with stop-scharm mixing.
 - Supersymmetry with sbottom-sstrange mixing.
3. Supersymmetry with flavor-violation from R-parity violating interactions:
 - Supersymmetry with trilinear R-parity violation.
 - Supersymmetry with trilinear and bilinear R-parity violation.

Folding in the existing experimental limits on the relevant parameter space of each of these models, we calculated the branching ratio for the decay $Z \rightarrow b\bar{s}$. The highlights of our results are summarized in Table VIII. In particular, we find that two Higgs doublet models with flavor violation originating from charged scalar interactions with fermions are expected to yield an extremely small $BR(Z \rightarrow b\bar{s})$; smaller than the SM prediction and smaller than the reach of a Giga-Z $\ell^+ \ell^-$ collider. Thus, a signal of $Z \rightarrow b\bar{s}$ in TESLA will be inconsistent with the underlying mechanisms for flavor violation in these two Higgs doublets model and will, therefore, rule out these options.

The same conclusions can be drawn in the stop-scharm mixing and the trilinear R-parity violation SUSY scenarios. On the other hand, SUSY with mixings between the bottom and strange-type squarks and/or mixings between sleptons and Higgs fields (bilinear R-parity violation) both of which may originate from the soft SUSY breaking sector, can drive the $BR(Z \rightarrow b\bar{s})$ to the 10^{-6} level for large $\tan\beta$ values. This enhancement is typical to these two flavor-violating SUSY scenarios if there are large mass-splittings between the scalars exchanged in the loops due to a GIM-like cancellation which is operational in the scalar mass-matrices and is, therefore, less effective as the scalar masses depart from degeneracy.

A $Z \rightarrow b\bar{s}$ signal in a Giga-Z TESLA or any other collider may, therefore, be a good indication for the underlying dynamics of these two flavor-violating SUSY scenarios and, if interpreted in that way, will provide for evidence of an hierarchical structure in the mass spectrum of the SUSY scalar sector.

Acknowledgments

G.E. and A.S. thank the U.S.-Israel Binational Science Foundation. G.E. also thanks the Israel Science Foundation and the Fund for Promotion of Research at the Technion for partial support. This work was also supported in part by US DOE Contract Nos. DE-FG02-94ER40817 (ISU) and DE-AC02-98CH10886 (BNL).

-
- [1] For a recent review on rare K , D and B decays, see e.g.: G. Isidori, hep-ph/0110225.
 - [2] For recent reviews on the experimental and theoretical status of rare top decays, see e.g.: B. Mele, hep-ph/0003064 and G.G. Hanson, hep-ex/0111058, respectively.
 - [3] M. Clements *et al.*, Phys. Rev. **D27**, 570 (1983); V. Ganapathi *et al.*, Phys. Rev. **D27**, 579 (1983); W.-S. Hou, N.G. Deshpande, G. Eilam and A. Soni, Phys. Rev. Lett. **57**, 1406 (1986); J. Bernabeu, M.B. Gavela and A. Santamaria, Phys. Rev. Lett. **57**, 1514 (1986).
 - [4] C. Busch, Nucl. Phys. **319**, 15 (1989); W.-S. Hou and R.G. Stuart, Phys. Lett. **B226**, 122 (1989); B. Grzadkowski, J.F. Gunion and P. Krawczyk, Phys. Lett. **268**, 106 (1991).
 - [5] B. Mukhopadhyaya and A. Raychaudhuri, Phys. Rev. **D39**, 280 (1989); see also M. J. Duncan, Phys. Rev. **D31**, 1139 (1985); F. Gabbiani, J.H. Kim and A. Masiero, Phys. Lett. **B214**, 398 (1988).
 - [6] M. Chemtob and G. Moreau, Phys. Rev. **D59**, 116012 (1999).
 - [7] W. Buchmüller and M. Gronau, Phys. Lett. **B220**, 641 (1989); G.T. Park and T.K. Kuo, Phys. Rev. **D42**, 3879, (1990); M.A. Perez and M.A. Soriano, Phys. Rev. **D46**, 284 (1992); J. Roldan, F.J. Botella and J. Vidal, Phys. Lett. **B283**, 389 (1992); X.-L. Wang, G.-R. Lu and Z.-J.

- Xiao, Phys. Rev. **D51**, 4992 (1995).
- [8] J. Fuster, F. Martinez-Vidal and P. Tortosa, preprint DELPHI 99-81 CONF 268, June 1999. Work presented at: “International Europhysics Conference on High-Energy Physics, Tampere, Finland, 15-21, July 1999-IOP, Bristol, 1999. Paper can be downloaded from: <http://documents.cern.ch/cgi-bin/setlink?base=preprint&categ=cern&id=open-99-393>.
- [9] D.E. Groom *et al.* (Particle Data Group), Euro. Phys. J. **C15**, 1 (2000).
- [10] A.D. Martin, R.G. Roberts, W.J. Stirling and R.S. Thorne, Eur. Phys. J **C14**, 133 (2000).
- [11] J.A. Aguilar-Saavedra *et al.*, (ECFA/DESY LC Physics Working Group), hep-ph/0106315.
- [12] C.M. Ankenbrandt, hep-ph/9901022.
- [13] D. Atwood, L. Reina and A. Soni, Phys. Rev. Lett. **75**, 3800 (1995); M. Sher, Phys. Lett. **B487**, 151 (2000).
- [14] See e.g., D. Atwood, S. Bar-Shalom, G. Eilam and A. Soni, Phys. Rep. **347**, 1 (2001) and references therein.
- [15] C.D. Froggatt, R.G. Moorhouse, I.G. Knowles, Nucl. Phys. **B386**, 63 (1992).
- [16] A.K. Das and C. Kao, Phys. Lett. bf B372, 106 (1996).
- [17] K. Kiers, A. Soni and G.-H. Wu, Phys. Rev. **D59**, 096001 (1999).
- [18] M. Ciuchini, G. Degrossi, P. Gambino and G.F. Giudice, Nucl. Phys. **B527**, 21 (1998). See also, P. Krawczyk and S. Pokorski, Phys. Rev. Lett. **60**, 182 (1988); J.L. Hewett, Proceedings of the SLAC Summer Inst. on Particle Physics: Spin Structure in High Energy Processes, Stanford, CA, 1993, hep-ph/9406302; Y. Grossman, H. Haber and Y. Nir, Phys. Lett. **B357**, 630 (1995); J.L. Hewett and J.D. Wells, Phys. Rev. **D55**, 5549 (1997).
- [19] G.-H. Wu and A. Soni, Phys. Rev. **D62**, 056005 (2000); K. Kiers, A. Soni and G.-H. Wu, Phys. Rev. **D62**, 116004 (2000).
- [20] M. Misiak, S. Pokorski and J. Rosiek, Adv. Ser. Direct. High Energy Phys. **15**, 795 (1998).
- [21] J.L. Diaz-Cruz, H.-J. He and C.-P. Yuan, hep-ph/0103178.
- [22] J. Rosiek, Phys. Rev. **D41**, 3464 (1990), unpublished Erratum in hep-ph/9511250.
- [23] F. Gabbiani, E. Gabrielli, A. Masiero and L. Silvestrini, Nucl. Phys. **B477**, 321 (1996); F. Borzumati, C. Greub and T. Hurth, Phys. Rev. **D62**, 075005 (2000); T. Besmer, C. Greub and T. Hurth, Nucl. Phys. **B609**, 359 (2001).
- [24] The curves in the figures end abruptly when the values of the parameter space involved is not compatible with our imposed restrictions from experimental data on the relevant physical quantities.
- [25] For reviews on R-parity violation see e.g., D.P. Roy, Pramana, J. Phys. **41**, S333 (1993), also in hep-ph/9303324; G. Bhattacharyya, Nucl. Phys. B (Proc. Suppl.) **52A**, 83 (1997); H. Dreiner, in *Perspectives in Supersymmetry*, edited by G.L. Kane (World Scientific, Singapore, 1998), hep-ph/9707435; P. Roy, “Seoul 1997, Pacific Particle Physics Phenomenology”, talk given at APCTP Workshop: Pacific Physics Phenomenology (P4 97), Seoul, Korea, 1997, hep-ph/9712520; S. Raychaudhuri, hep-ph/9905576.
- [26] Y. Grossman and H.E. Haber, Phys. Rev. **D59**, 093008 (1999).
- [27] S. Roy and B. Mukhopadhyaya, Phys. Rev. **D55**, 7020 (1997); M.A. Diaz, J.C. Romao and J.W.F. Valle, Nucl. Phys. **B524**, 23 (1998); C.-h. Chang and T.-f. Feng, hep-ph/9908295; B. Mukhopadhyaya and S. Roy, Phys. Rev. **D60**, 115012 (1999).
- [28] S. Davidson, M. Losada and N. Rius, Nucl. Phys. **B587**, 118 (2000).
- [29] See e.g., K. Choi, E.J. Chun and K. Hwang, Phys. Lett. **B488**, 145 (2000).
- [30] M. Bisset, O.C.W. Kong, C. Macesanu and L.H. Orr, Phys. Rev. **D62**, 035001 (2000).
- [31] See e.g., H.-P. Nilles and N. Polonsky, Nucl. Phys. **B484**, 33 (1997); B. Mukhopadhyaya, S. Roy and F. Vissani, Phys. Lett. **B443**, 191 (1998); M. Hirsch, M.A. Diaz, W. Porod, J.C. Romao and J.W.F. Valle, Phys. Rev. **D62**, 113008 (2000).
- [32] J. Ferrandis, Phys. Rev. **D60**, 095012 (1999).
- [33] For a list of updated bounds on the $\lambda'\lambda'$ products that enter the radiative decay $Z \rightarrow b\bar{s}$ see G. Bhattacharyya, D. Chang, C.-H. Chou and W.-Y. Keung, Phys. Lett. **B493**, 113 (2000).
- [34] B. de Carlos and P.L. White, Phys. Rev. **D55**, 4222 (1997); T. Besmer and A. Steffen, Phys. Rev. **D63**, 055007 (2001).
- [35] Y. Grossman and H.E. Haber, Phys. Rev. **D63**, 075011 (2001); S. Davidson and M. Losada, hep-ph/0010325.
- [36] S. Bar-Shalom, G. Eilam and B. Mele, Phys. Lett. **B500**, 297 (2001).
- [37] S. Bar-Shalom, G. Eilam and B. Mele, Phys. Rev. **D64**, 095008 (2001).
- [38] See e.g., talks given by Tom Junk at the “LEP Fest”, 10 October 2000, and by P. Teixeira-Dias, 10 July 2001, in <http://lephiggs.web.cern.ch/LEPHIGGS/talks>.
- [39] S. Heinemeyer, W. Hollik and G. Weiglein, hep-ph/0002213.
- [40] G. Bhattacharyya, J. Ellis and K. Sridhar, Mod. Phys. Lett. **A10**, 1583 (1995).
- [41] B. Allnsch *et al.*, hep-ph/9906224, edited by H. Dreiner.
- [42] For the FF package that was used for numerical evaluation of the loop integrals see: G.J. van Oldenborgh, Comput. Phys. Commun. **66**, 1 (1991). For the algorithms used in the FF package see: G.J. van Oldenborgh and J.A.M. Vermaseren, Z. Phys. **C46**, 425 (1990).
- [43] G. Passarino and M. Veltman, Nucl. Phys. **B160**, 151 (1979).

APPENDIX A: ONE-LOOP FORM FACTORS

In this appendix we give the two-point and three-point one-loop form factors which are defined by the one-loop momentum integrals as follows [42]:

$$C_0; C_\mu; C_{\mu\nu}(m_1^2, m_2^2, m_3^2, p_1^2, p_2^2, p_3^2) \equiv \int \frac{d^4q}{i\pi^2} \frac{1; q_\mu; q_\mu q_\nu}{[q^2 - m_1^2][(q + p_1)^2 - m_2^2][(q - p_3)^2 - m_3^2]}, \quad (\text{A1})$$

$$\tilde{C}_0; \tilde{C}_\mu (m_1^2, m_2^2, m_3^2, p_1^2, p_2^2, p_3^2) \equiv \int \frac{d^4 q}{i\pi^2} \frac{q^2; q^2 q_\mu}{[q^2 - m_1^2] [(q + p_1)^2 - m_2^2] [(q - p_3)^2 - m_3^2]} , \quad (\text{A2})$$

$$B_0; B_\mu (m_1^2, m_2^2, p^2) \equiv \int \frac{d^4 q}{i\pi^2} \frac{1; q_\mu}{[q^2 - m_1^2] [(q + p)^2 - m_2^2]} , \quad (\text{A3})$$

where $\sum_i p_i = 0$ is to be understood above.

The coefficients B_x with $x \in 0, 1$, C_x with $x \in 0, 11, 12, 21, 22, 23, 24$ and \tilde{C}_x with $x \in 0, 11, 12$ are then defined through the following relations [43]:

$$\tilde{C}_\mu = p_{1\mu} \tilde{C}_{11} + p_{2\mu} \tilde{C}_{12} , \quad (\text{A6})$$

and

$$B_\mu = p_\mu B_1 , \quad (\text{A4})$$

$$C_\mu = p_{1\mu} C_{11} + p_{2\mu} C_{12} , \quad (\text{A5})$$

$$C_{\mu\nu} = p_{1\mu} p_{1\nu} C_{21} + p_{2\mu} p_{2\nu} C_{22} + \{p_1 p_2\}_{\mu\nu} C_{23} + g_{\mu\nu} C_{24} , \quad (\text{A7})$$

where $\{ab\}_{\mu\nu} \equiv a_\mu b_\nu + a_\nu b_\mu$.